BNWL-SA-2412

Unclass
J Sahm 9/25/69

[redacted]

VIBRATIONALLY COMPACTED CERAMIC FUELS

FEBRUARY 1969

[redacted]

BATTELLE NORTHWEST
BATTELLE MEMORIAL INSTITUTE PACIFIC NORTHWEST LABORATORY
BATTELLE BOULEVARD, P. O. BOX 999, RICHLAND, WASHINGTON 99352

BNWL-SA-2412

DISCLAIMER

LEGAL NOTICE

PACIFIC NORTHWEST LABORATORY
RICHLAND, WASHINGTON
operated by
BATTELLE MEMORIAL INSTITUTE
for the
UNITED STATES ATOMIC ENERGY COMMISSION UNDER CONTRACT AT(45-1)-1830

AEC-RL RICHLAND, WASH.

BNWL-SA-2412

VIBRATIONALLY COMPACTED CERAMIC FUELS

M. D. Freshley

and

T. B. Burley

Battelle Memorial Institute
Pacific Northwest Laboratory
Richland, Washington

February 1969

This paper is based on work performed under United States Atomic Energy Commission Contract AT(45-1)-1830.

TABLE OF CONTENTS

		Page
I.	Introduction	1
II.	Summary	2
III.	Process Variables	4
IV.	Fabrication Process	6
	Powder Preparation	6
	Vibrational Compaction	8
V.	Irradiation Behavior	10
	PRTR Experience	10
	Effective Thermal Conductivity	13
	Structure Alteration	14
	Fission Product Migration	26
	Fission Gas Release	31
VI.	Defect Behavior	40
	Intentionally Defected Experiments	41
	PRTR In-Service Defects	44
VII.	Transient Behavior	46
	References	51

VIBRATIONALLY COMPACTED CERAMIC FUELS

M. D. Freshley and T. B. Burley

I. Introduction

The effects of vibration on the packing of powder particles have been studied in detail, theoretically as well as experimentally. Vibratory compacting of powders plays an important role in many industries, and a specialized adaptation of the process has been successfully applied to the fabrication of ceramic fuel elements for nuclear reactors. The development of vibrationally compacted ceramic fuels was initiated at the Pacific Northwest Laboratory in 1959[1] and has been continued since that time by numerous investigators throughout the world. The reliable irradiation performance of vibrationally compacted ceramic fuels operating under advanced power reactor conditions has been demonstrated; however, like other types of ceramic fuels, control of process variables during fabrication must be given careful attention. Vibrational compaction techniques have been successfully applied to various fuel materials, different cladding materials, and various fuel geometries for both thermal[2,3] and fast reactor[4] applications.

Interest in the vibrational compaction process, which was an outgrowth of swage compaction, has been stimulated by its inherent simplicity and versatility. Initially, emphasis on developing vibrationally compacted fuel technology was motivated primarily by potential economic factors.

Although comparative cost studies indicate that, based upon existing fabrication technology, there is no significant difference between vibrational compaction and the more conventional pelletizing processes[5,6], vibrational compaction probably offers the greatest potential for economic gains even with simple rod

configurations. For instance, the perfection of low cost feed materials suitable for vibrational compaction, particularly mixed oxides, may significantly enhance the potential of the process. The potential advantages of vibrational compaction as a versatile fuel fabrication process suitable for complex fuel element configurations, a variety of fuel materials, and adaption to remote handling are generally recognized.

The incentives for vibrational compaction may well increase with advances in fuel technology and the resulting increase in performance requirements. Vibrationally compacted fuels may have decided advantages for the high power-high burnup operation anticipated for future power reactors where the effects of core-clad interactions and the accommodation of swelling become important fuel performance considerations.

II. Summary

Interest in vibrationally compacted nuclear fuels has been stimulated by the inherent simplicity and versatility of the process and the possibility that the process offers the greatest potential for economic gains. The vibrational compaction process has been successfully applied to different types of fuel materials.

The compaction efficiency achieved during vibrational compaction is affected by particle characteristics and compaction techniques. Densities in the range of 85 to 88% TD can be readily attained in full-sized rods using three particle size fractions. A fabrication process utilizing high-energy-rate pneumatically impacted UO_2-PuO_2 fuel material was used at PNL in the development of packed-particle mixed-oxide fuels suitable for plutonium recycle in thermal reactors.

Vibrationally compacted ceramic fuels have been successfully irradiated in PRTR, EBWR, and commercial BWR's and PWR's to peak burnups of nearly 34,000 MWd/MTM. Irradiations in PRTR are being conducted at peak power generations of nearly 20 kW/ft with maximum fuel temperatures near melting. Peak burnups in PRTR are over 18,000 MWd/MTM.

Fuel melting occurs in 86% TD vibrationally compacted UO_2-2 wt% PuO_2 fuel rods at a linear rod power of 655 ± 15 w/cm under PRTR conditions which is equivalent to a thermal conductivity integral value of 50 w/cm. In-reactor sintering and densification of the fuel causes restructuring to occur relatively rapidly during irradiation although time-temperature dependent sintering effects cause more subtle structural changes to occur.

During extended exposures, data indicate that the in-reactor columnar grain growth temperature in pneumatically impacted UO_2-PuO_2 fuel is approximately 1800 ^{o}C. The indicated sintering temperature is approximately 1700 ^{o}C although there is some apparently anomalous data that indicate the in-reactor sintering temperature may be as low as 1100-1200 ^{o}C in high burnup fuel rods.

The internal pressure in vibrationally compacted fuel rods during irradiation is less than expected although the rate of pressure buildup is consistent with predicted gas release fractions. Fission gas release is independent of burnup or burnup rate to peak burnups of nearly 10,000 MWd/MTM.

The defect behavior of vibrationally compacted oxide fuel operating at heat ratings employed in power reactors has been satisfactory. There is some evidence which indicates that the defect behavior mode may change in the range of 800 to 900 w/cm with considerable fuel melting and could become the limiting criterion for advanced or very high power operation.

Limited data on the transient behavior of vibrationally compacted fuels indicate that there may be significant differences between vibrationally compacted and pellet-containing fuel rods. There are indications that the failure modes of vibrationally compacted and pellet-containing fuels are different, although the failure threshold values are comparable, and that meltdown transients of vibrationally compacted fuels result in higher and more rapid pressure pulses than pellet-containing fuels. However, more data are needed to better define the transient behavior of vibrationally compacted fuels.

III. Process Variables

The packing efficiency achieved during vibrational compaction of nuclear fuels is affected by the particle characteristics and the compaction procedures[2]. The particle characteristics that principally affect the packing efficiency and possibly the uniformity of vibrationally compacted rods are density, size distribution, and shape. Other factors include segregation by size and shape, ratio of the container diameter to particle diameter or wall effect, hardness, and surface area of irregular shaped particles of crushed fuel material. Compaction procedures which primarily affect packing efficiency are characteristics of the applied vibration (frequency and acceleration of applied vibration), loading techniques, and compaction time.

Theoretical[7] and experimental[8] investigations of idealized systems have been conducted which serve as guides for (1) selecting the proper particle size distributions to achieve high density fuel compacts of various geometric configurations and (2) permitting maximum utilization of starting material. Because the particle diameters specified by the models can only be approximated by screening and because of other difficult to define variables such as particle shape, some empirical evaluation is required to achieve the maximum packing efficiency. In applying vibrational compaction techniques, the interrelationship of the various independent variables must be empirically optimized to obtain the desired result.

Because high density fuel particles are necessary for vibrational compaction processes aimed at high bulk densities, various types of high density feed materials have been used. These include sintered and crushed, fused, electrodeposited, Sol-Gel, and pneumatically impacted fuel material. The high density particles also provide improved fission gas retention and higher thermal conductivity.

Although densities up to 95% of theoretical have been attained in idealized systems with a minimum of applied energy[8], densities in the range of 85 to 88% TD can be readily attained in full-sized fuel rods using three particle size fractions of crushed oxide fuel particles in a reasonable compaction time without damage to the cladding. The optimum particle size distribution for any given application may vary depending upon the independent variables; however, it usually falls within the limits of 50% to 65% coarse, 10% to 35% medium, and 15% to 30% fine. A commonly used particle size distribution of the fuel is 55% -6+10 mesh, 25% -20+65 mesh, and 20% -200 mesh. A 1.27 cm diameter PRTR fuel rod with an active fuel length of 58 inches can be loaded with approximately 2 Kg of pneumatically impacted fuel to 85-87% TD in two to three minutes[2].

Vibratory feeders and small conveyors have been used during simultaneous loading and compacting of homogeneously enriched fuel to prevent bridging in long fuel rods. Conveyors have the possible advantage of providing better control of the particle size distribution of fuel as it enters the tube. Other techniques such as incremental loading are used in loading "heterogeneously" enriched UO_2-PuO_2 fuels in which the PuO_2 is contained in the fine particle size fraction[9].

Various types of equipment including high-impact pneumatic vibrators, ultrasonic devices, and electrodynamic equipment are used for vibrationally compacting nuclear fuels[10]. High compaction efficiencies can be achieved using either electrodynamic or pneumatic vibration equipment. Variable frequency electrodynamic vibrators provide greater versatility for different fuel element designs. For established fabrication processes, however, pneumatic vibrators which are less versatile but less expensive may be more practical. Best results were obtained at PNL by simultaneous loading and compaction at frequencies that were rapidly varied over a range of several kilocycles. Densification was enhanced by the excitation of several resonant frequencies in rods which were rigidly coupled to the vibrator[2].

IV. Fabrication Process

Fuel studies at PNL have been concerned principally with the development of packed-particle mixed-oxide fuels suitable for plutonium recycle in thermal power reactors. The first mixed oxide fuels were made by incremental loading or mechanically mixing UO_2 and PuO_2 powders to obtain a relatively uniform gross axial distribution of PuO_2 in vibrationally compacted rods[9]. Moderate layering of the PuO_2 occurred within increments during loading, and gamma scanning techniques were used to assure that no hot spots caused by local concentrations of plutonium would exceed the maximum permissible point heat flux limit in the Plutonium Recycle Test Reactor (PRTR).

Subsequently, a fabrication process utilizing high-energy-rate pneumatically impacted UO_2-PuO_2 fuel material was used to fabricate elements for PRTR and other reactors including the Experimental Boiling Water Reactor and Saxton (Figure 1).[11] The principal features of the process are the techniques for preparing and vibrationally compacting the high density,mixed-oxide fuel particles.

Powder Preparation

Pneumatic impaction provides a means of producing high density UO_2-PuO_2 fuel particles with any desired PuO_2 composition suitable for vibrational compaction.[11] Appropriate particle sizes and proportions of UO_2 and PuO_2 powders are mechanically blended prior to loading into a double stainless steel can assembly which contains about 6 Kg of fuel. After vacuum outgassing at 1200 ^{o}C, the assembly is impacted at peak pressures as high as 1.76×10^{8} Kg/m^2 (250,000 lb/in^2) in a high energy rate forging machine. As much as 145,000 ft-lb of work can be delivered to the fuel during the impact time of several milliseconds. After impaction, the high density, mixed-oxide is pulverized and mechanically sieved into the different size fractions suitable for vibrational compaction.

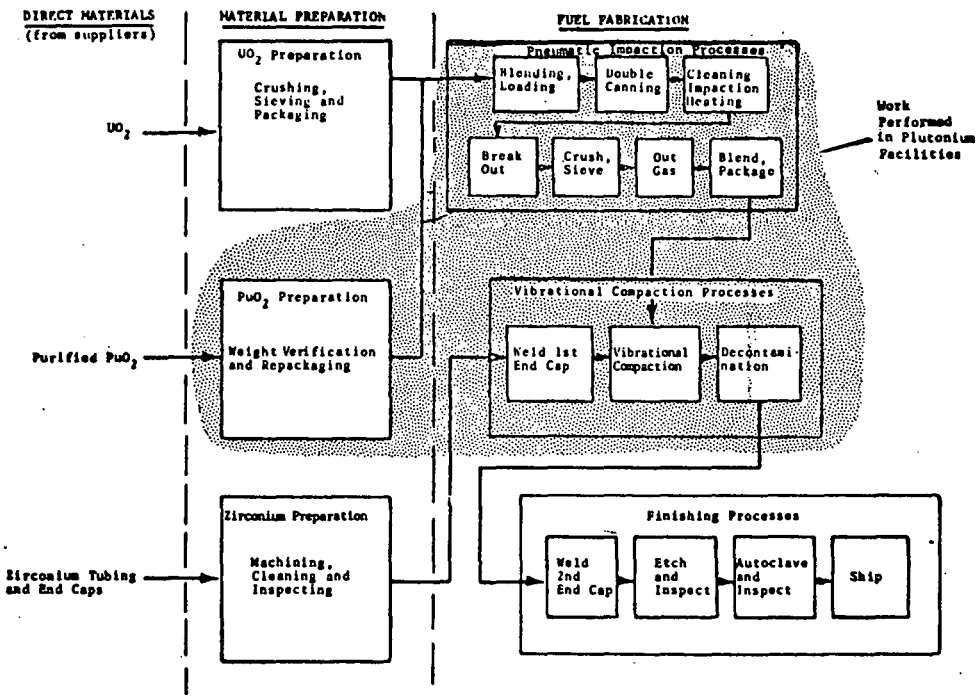

Figure 1. Fabrication of UO_2-PuO_2 Fuel Rods by Pneumatic Impaction-Vibrational Compaction.

Control of oxygen/metal ratio and sorbed gas content of the pre-impacted powders are important factors in obtaining high density fuel material. Slightly hyperstoichiometric UO_2-PuO_2 feed material is required for the impaction process because excess oxygen enhances plasticity and produces higher impacted fuel densities. Mixed-oxide particle densities of >98% TD are obtained routinely with material having an O/M ratio of 2.02.

Oxide fuel materials have an affinity for moisture and the problem of moisture pickup is accentuated with pulverized powders. Moisture in powder fuel can be successfully controlled by employing vacuum outgassing techniques, handling the outgassed powders in dry inert atmospheres, and minimizing the time between the outgassing and loading operations. Pulverized mixed-oxide fuel material for PRTR is vacuum outgassed at 250 ^{o}C for at least two hours at a pressure no greater than 10^{-3} torr immediately prior to loading to drive of residual hydrocarbons, moisture, and gas.[12] Subsequent handling is performed in nitrogen filled glove boxes in which the relative humidity is controlled at 2-5%. The moisture content of the powder processed in this manner is in the range of 20 to 40 ppm (2 to 5 ppm hydrogen) with a sorbed gas content of about 0.07 cm^3/g.[13] In addition to vacuum outgassing the powders prior to loading, some investigators have resorted to baking the compacted fuel assembly in a vacuum drying retort to reduce the hydrogen concentration in the fuel to a level of 3-8 ppm.[14] This operation appears to be an unnecessary precaution.

Vibrational Compaction

A pre-weighed amount of fuel is loaded continuously into the tube by means of a vibratory feeder during compaction[2]. The tube is vibrated at frequencies that are continously varied between 250 and 750 cps at an acceleration of approximately 30 G's during a loading time of approximately 1-1/2 minute. After loading, higher levels of applied vibration (nearly 50 G's) are utilized until the fuel assumes a specified height in the cladding tube. Loading and compacting PRTR UO_2-PuO_2 fuel roads to densities of 85 to 87% TD is routinely performed in 2 to 3 minutes.

Specially developed, highly sensitive ultrasonic testing techniques were used to detect small fatigue-type cracks in the weld area caused by the vibrational energy of one group of fuel rods.[15] The cause of the cracks was attributed to improper mechanical coupling of the rod to the vibrator and excessive compaction times. Correction of these problems eliminated the cracking.

Most fuel fabrication processes include autoclaving the Zircaloy cladding in steam at temperatures of approximately 400 ^{o}C for up to 48 hours. Some fuel fabrication processes specify autoclaving the inside and outside surfaces of the Zircaloy cladding tubing prior to fuel loading whereas, others, such as the process used at PNL, specify that autoclaving be performed after the fuel rods are loaded and sealed. The particular technique used could have a pronounced effect on the hydriding behavior of the cladding from the moisture trapped within the rod. The thick oxide layer on pre-autoclaved tubing could develop small imperfections during loading which are susceptible to localized massive hydriding from relatively small amounts of water trapped in the fuel. In non-pre-autoclaved rods, however, air and moisture trapped within vibrationally compacted fuel rods react with the cladding to form a uniform thin ZrO_2 layer on the inside surface during autoclaving. As the available oxygen is consumed by the cladding, the ZrO_2 layer becomes permeable to hydrogen; however, the hydrogen absorption in this case should be more uniform. It has been reported, however, that the presence of oxide films on the surface of Zircaloy localized the absorption because hydrogen diffused through some areas of the film much faster than through others.[16] This is possibly caused by localized variations in the texture or composition of the base metal. The conditions under which internally trapped hydrogen reacts with the Zircaloy cladding to form localized massively hydrided regions or homogeneous layers during irradiation requires further investigation.

V. Irradiation Behavior

PRTR Experience

Vibrationally compacted UO_2 and UO_2-PuO_2 fuels have been irradiated in PRTR, EBWR, and commercial BWR's and PWR's to peak burnups of nearly 34,000 MWd/MTM (Table I). Additionally, a large number of vibrationally compacted capsules and prototype fuel assemblies have been irradiated over a wide range of conditions by various laboratories throughout the world.

TABLE I

Vibrationally Compacted Fuel Irradiations

Reactor	Approximate No. of Rods	Fuel	Approx. Peak Power, w/cm	Approx. Peak B.U., MWd/MTM
PRTR	2242	UO_2-PuO_2	690	18,500
EBWR	1296	UO_2-PuO_2	328	3,400
Saxton	148	UO_2-PuO_2	525	33,800

Over 120 vibrationally compacted 19-rod cluster elements containing UO_2-PuO_2 fuel have been irradiated in PRTR (Figure 2)[17,18]. These irradiations are providing statistically significant performance data on plutonium-containing fuels operated at power generations and to goal burnups greater than those currently employed in commercial power reactors. Actual maximum linear rod power generations are nearly 655 w/cm (20 kW/ft) with maximum fuel temperatures near melting, and maximum goal burnups are in the range of 45,000 MWd/MTM. Vibrationally compacted mixed oxide fuel elements being irradiated in the PRTR as part of the Batch Core Experiment* have reached peak burnups of 11,000 MWd/MTM[19]. Included in the 66 High Power Density (HPD) fuel elements comprising the Batch Core are vibrationally compacted powder, hot pressed pellet, and cold pressed and sintered UO_2-PuO_2 pellet fuels. Pneumatically impacted, vibrationally compacted UO_2-PuO_2 HPD fuel elements continue to perform satisfactorily; no failures have occurred. The burnup status of the HPD elements in the Batch

*The purpose of the Batch Core Experiment in PRTR is to evaluate the physics parameters of a plutonium enriched fuel loading as a function of burnup under controlled conditions. The vibrationally compacted HPD elements used in the Batch Core Experiment are designed to operate at an actual peak rod power generation of 890 w/cm (27 kW/ft) to peak burnups of over 45,000 MWd/MTM.

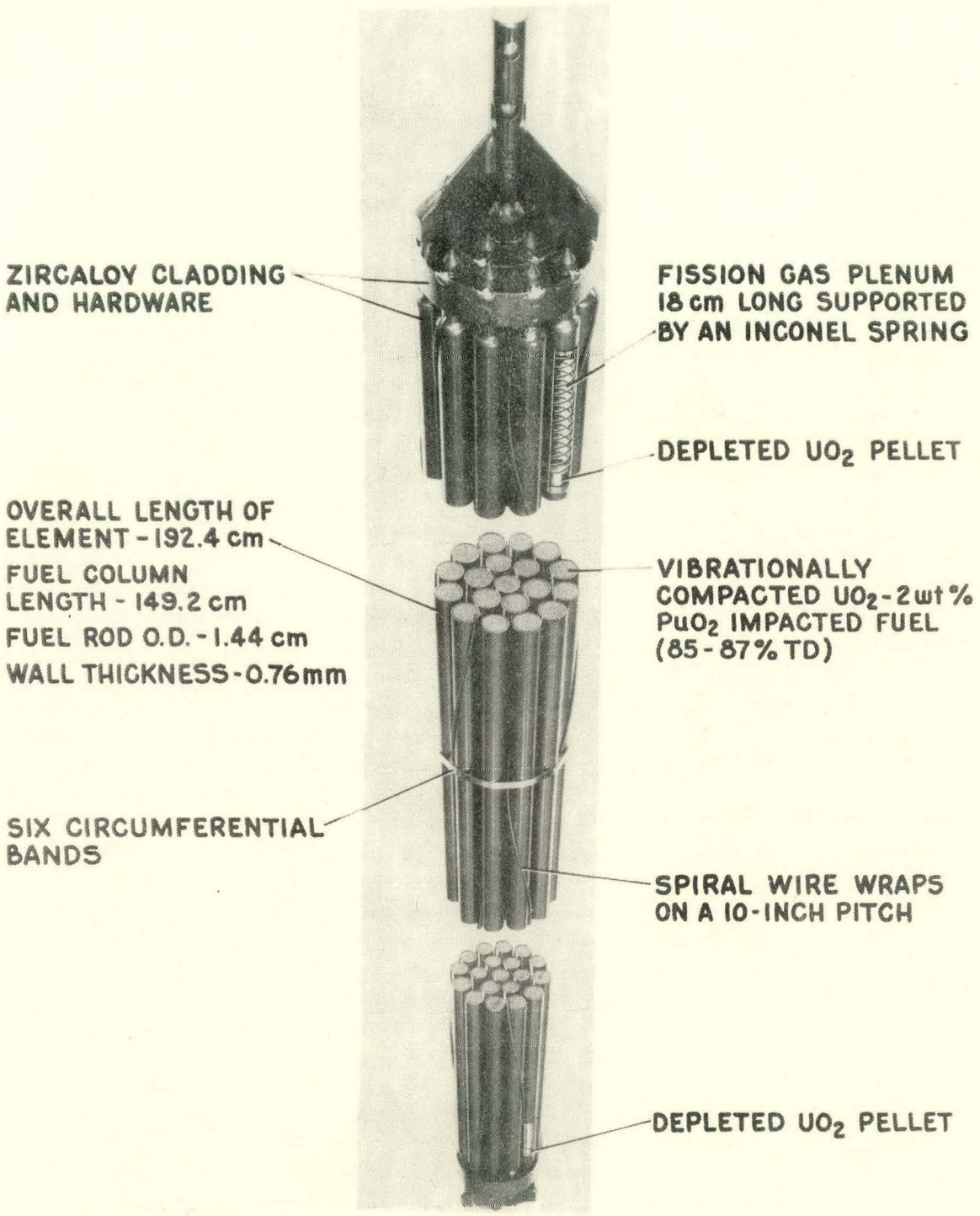

Figure 2

PRTR High Power Density
Nineteen-Rod Cluster Fuel Element

Core is summarized in Table II. To meet the performance criteria of presently designed PWR-BWR fuels, irradiation of 12 to 19 selected UO_2-PuO_2 HPD fuel assemblies will be continued to peak burnups of about 45,000 MWd/MTM after the Batch Core Experiment has been completed.

Swaged and vibrationally compacted elements which contain pneumatically impacted and mechanically mixed (incrementally loaded) UO_2-PuO_2 type fuel have now achieved peak burnups of over 18,500 MWd/MTM in the fringe positions of PRTR[19]. Their performance continues to be excellent.

TABLE II

PRTR Core Loading Status
January 1, 1969

Element Type[a]	Number of Elements	Actual Peak Rod Power Gen., w/cm (kW/ft)	Peak Burnup, MWd/MTM
Batch Core Experiments			
Vipac PI[b] UO_2-2 wt% PuO_2 (Batch Core Experimental Elements)	64	655 (20)	11,000
Commercial UO_2-1.94 wt% PuO_2 Pellet Fuel (Hot Pressed and Cold Pressed and Sintered)	2	690 (21)	10,000
8-Rod FERTF Test Element	1	590 (>18)	--
Fringe Position Tests			
Vipac PI UO_2-2 wt% PuO_2 (Pilot HPD Elements)	6	655 (20)	13,000
Swaged PI UO_2-2 wt% PuO_2	1	655 (20)	8,500
Swaged PI UO_2-1 wt% PuO_2	1	558 (17)	14,000
Vipac PI UO_2-1 wt% PuO_2	2	492 (15)	11,500
Vipac MM[c] UO_2-0.5 wt% PuO_2	1	525 (16)	18,500
Swaged MM UO_2-0.5 wt% PuO_2	2	426 (13)	17,000
Swaged UO_2	1	460 (14)	15,000

(a) PRTR elements are 19-rod clusters of 0.565-inch OD Zircaloy-clad rods with active fuel lengths of 58.5 and 88.5.
(b) PI = High-energy-rate pneumatically impacted fuel.
(c) MM = Mechanically mixed fuel.

Routine underwater examination of the PRTR fuel elements indicates that, in general, their condition is excellent. Minor damage in the form of broken circumferential strip bands, broken rod wire wraps, and bent hanger pins are repaired to permit continued irradiation of the elements. A thin layer of crud deposits on the rods during irradiation in the neutral pH coolant, however, there is some evidence that localized removal is occurring. The rate of crud formation is not expected to pose any serious operating problem.

Rod wire wraps on some of the long term elements have loosened. The loosening is probably a result of plastic yielding of the wire caused by differential thermal expansion between the wire and the hotter rod. There is no evidence of fretting or crud removal associated with the loose wires -- thus indicating that the spacing wires probably tighten during operation.

Effective Thermal Conductivity

Experience has shown that fuel melting occurs in 86% TD vibrationally compacted UO_2-2 wt% PuO_2 fuel rods at a linear rod power of 655 ± 15 w/cm (20 ± 0.5 kW/ft) under PRTR operating conditions. (The power generation required to produce the onset of fuel melting is subject to refinement as more data are acquired.) This is equivalent to an $\int_{T_s}^{T_m} K d\phi$ of 50 w/cm where:

T_s = Temperature of fuel surface
= ∿ 530 °C

T_m = Temperature of fuel melting
= ∿ 2800 °C

K = Thermal conductivity of fuel

ϕ = Temperature

Since the power to produce melting was determined with relatively low exposure fuel rods, the value of the conductivity integral would tend to increase with increasing fuel burnup as a result of time-temperature dependent sintering effects. Definition of an appropriate thermal conductivity curve for vibrationally compacted fuel is difficult because the effect of the time-temperature dependent changes is unknown and the sintering behavior is not necessarily consistent.

The value of 50 w/cm is in good agreement with the value of 49 w/cm for vibrationally compacted UO_2 published by Lyons, et al.[20] This data indicates that the thermal conductivity of dilute UO_2-PuO_2 fuel is essentially the same as for UO_2 fuels, as expected, and that the power to produce melting in vibrationally compacted fuels is about 20% less than for high density sintered pellet fuel. The shape of the thermal conductivity curve for vibrationally compacted fuel needs further refinement although, fuel temperature calculations made using the curve presented by Lyons, et al,[20] seem to provide a reasonably accurate indication of the operating conditions during irradiation. The conductivity curve and the calculations indicate that after the initial sintering and densification, most of which occurs rapidly during irradiation, the conductivity of the fuel operating above the grain growth temperature approaches the conductivity of high density sintered pellets. The difference in effective conductivity and in the conductivity integral values from surface to melting between powder and pellets is attributable to the poorer conductivity of the unsintered fuel operating below grain growth temperatures which persists at the periphery.

Structure Alteration

The structure of vibrationally compacted mixed-oxide fuel changes dramatically during irradiation and the degree of alteration depends upon the irradiation conditions, power history, and exposure (Figure 3). Irradiation alteration affects the behavior of the fuel by changing the spatial position within the rod, the effective thermal conductivity, fission product distribution, and failure behavior. In-reactor sintering and densification of the fuel cause a central void to form in the thermal center. A wide band of radially oriented columnar grains surrounds the central void which, in turn, is surrounded by a narrow region of equiaxed grain growth. Although most of the fuel restructuring occurs relatively rapidly during irradiation, time-temperature dependent sintering effects cause the sintering boundary radius to increase with exposure. Refinement of the columnar grains also occurs during extended

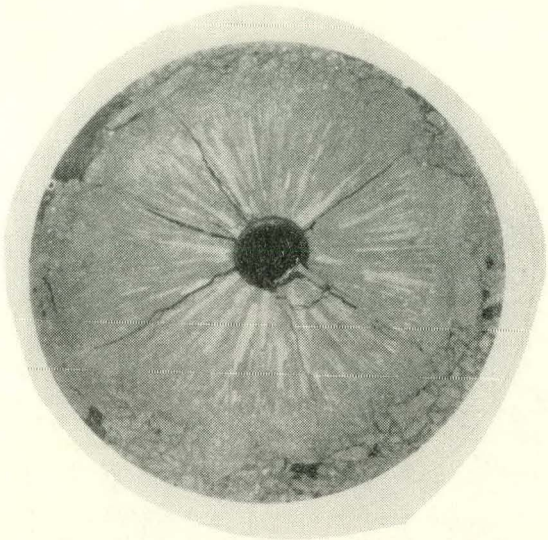

1350 MWd/MTM

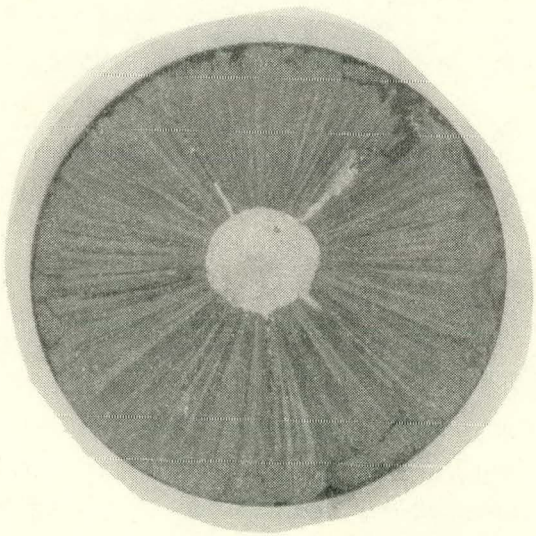

4950 MWd/MTM

Figure 3

Transverse Sections of PRTR Vibrationally Compacted UO_2-2 wt% PuO_2 Fuel Rods Irradiated at a Linear Rod Power Near 655 w/cm (20 kW/ft).

exposures and, in general, the fuel structures become more uniform with fewer localized discontinuities. Postirradiation fuel structures represent only the latter stages of irradiation because it has been shown that once-molten fuel structures formed during irradiation can be erased by time-temperature dependent diffusion phenomena in less than 72 hours irradiation under nonmolten, but high temperature conditions.[18]

In-reactor homogenization and solid-solution formation by UO_2 and PuO_2 interdiffusion starts in pneumatically impacted fuel at temperatures sufficient to cause sintering or equiaxed grain growth, and it occurs relatively rapidly at the higher irradiation temperatures. The close consolidation of the pneumatically impacted UO_2 and the small (-325 mesh) PuO_2 particles enhance the homogenizing process. Homogenization of the UO_2-PuO_2 fuel is apparent, on beta-gamma and alpha-autoradiographs* by the lack of resolution of localized concentrations of fission products associated with discrete PuO_2 particles.

---

* The beta-gamma autoradiographs described in this paper were made by exposing irradiated specimens to high resolution film plates which, after developing, indicate fission products. The alpha-autoradiographs were made by exposing irradiated specimens to cellulose acetate, which, after etching in sodium hydroxide, indicate plutonium or alpha emitting isotopes associated with plutonium. Dark areas on both types of autoradiographs correspond to regions of high activity. Alpha energy analysis of microdrilled samples shows that approximately 32% of the total activity is caused by alpha-energies normally associated with ^{242}Cm. The remainder of the alpha activity is principally from plutonium isotopes and ^{241}Am although there was no significant amount of ^{241}Am in the samples. Curium^{242} is associated with plutonium-originally included as enrichment material, plus that formed from ^{238}U because uranium decay chains modified by neutron reactions do not result in the formation of significant amounts of Cm. Curium^{242} is formed by the beta decay of ^{242}Am which is formed by neutron capture in ^{241}Am, a daughter product via beta decay of ^{241}Pu.

Melting in irradiated mixed oxide fuel rods is evidenced by the formation of a well defined region in the thermal center of the fuel: a region composed of a cellular or sometimes porous appearing subgrain structure (Figure 4). A band of pore-free high density grains, often characterized by a circumferential laminar appearing structure, is outside the well defined porous fuel region. The remaining structure is similar to that described for the nonmolten condition. The once-molten region at the time of shutdown is also delineated on the beta-gamma autoradiograph by the centrally located region of uniformly high fission product concentration. The boundary of the high plutonium concentration region indicated on the alpha autoradiograph does not necessarily correspond to the terminally molten fuel region. The alpha autoradiograph indicates that the initial molten fuel boundary possibly extended to the outer edge of the high density band. An increasing effective thermal conductivity, caused by in-reactor sintering of lower temperature fuel, would cause the molten boundary to recede. A receding molten boundary is suggested by the laminar rings often observed in the high density band.

Postirradiation examination of PRTR fuel rods that have operated with molten fuel shows that the diameter of the central void in the upper parts of rods is generally larger than it is below the midplane of the fuel column. In the upper regions, evidence of once-molten fuel is generally found only on the inner surface of the central void. In the lower regions, one finds essentially no central void. This illustrates gravitational settling of molten fuel because the axial flux distribution was essentially symmetrical about the midplane.

Three transverse sections were examined from a pneumatically impacted, vibrationally compacted UO_2-2 wt% PuO_2 PRTR fuel rod with a peak burnup of 7800 MWd/MTM. The fuel rod operated at a nominal peak power generation of 590 w/cm (18 kW/ft). A central void and radially oriented columnar grains to 63% of the radius formed in the transverse section from the peak power position (Figure 5). This structure is in good agreement with the

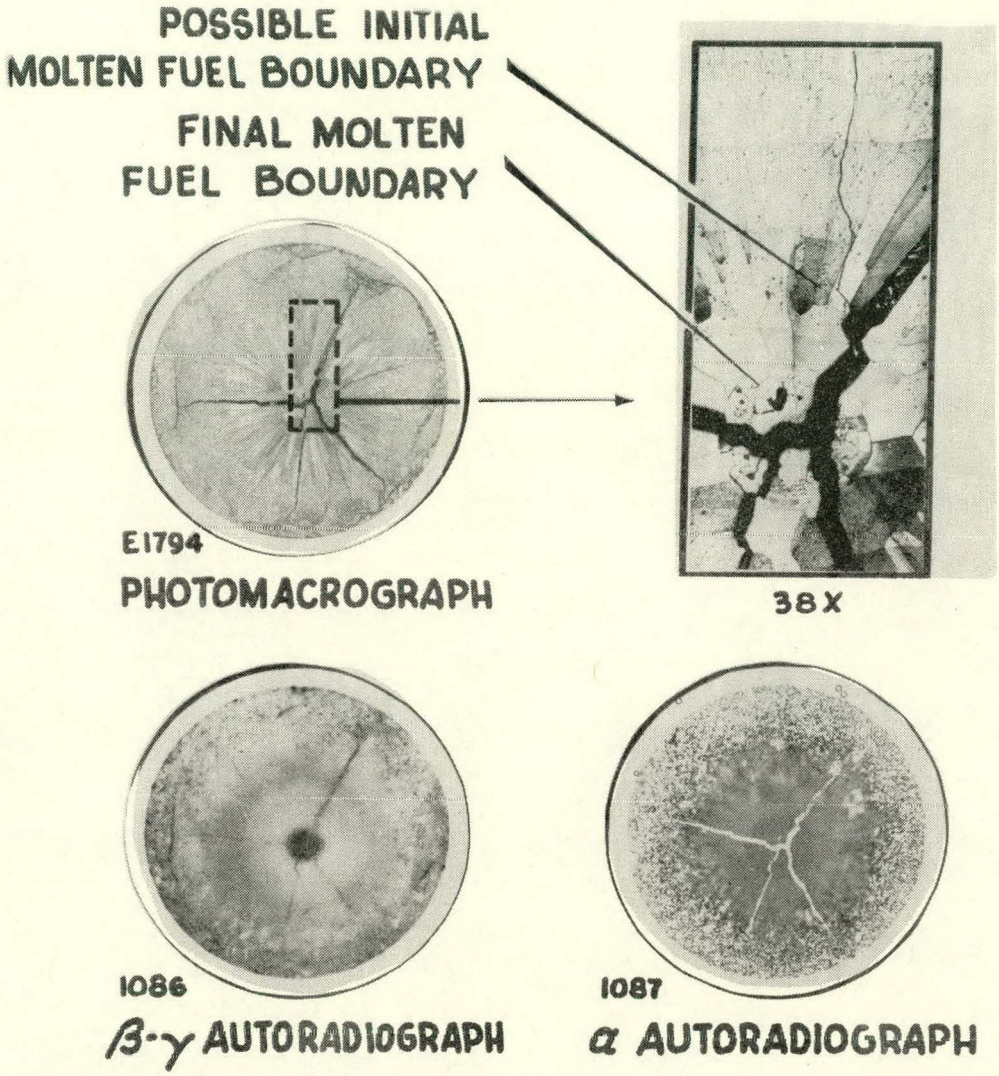

Figure 4

Transverse Section of a PRTR Vibrationally Compacted UO_2-2 wt% PuO_2 Fuel Rod Irradiated at a Linear Rod Power of Approximately 690 w/cm (21 kW/ft).

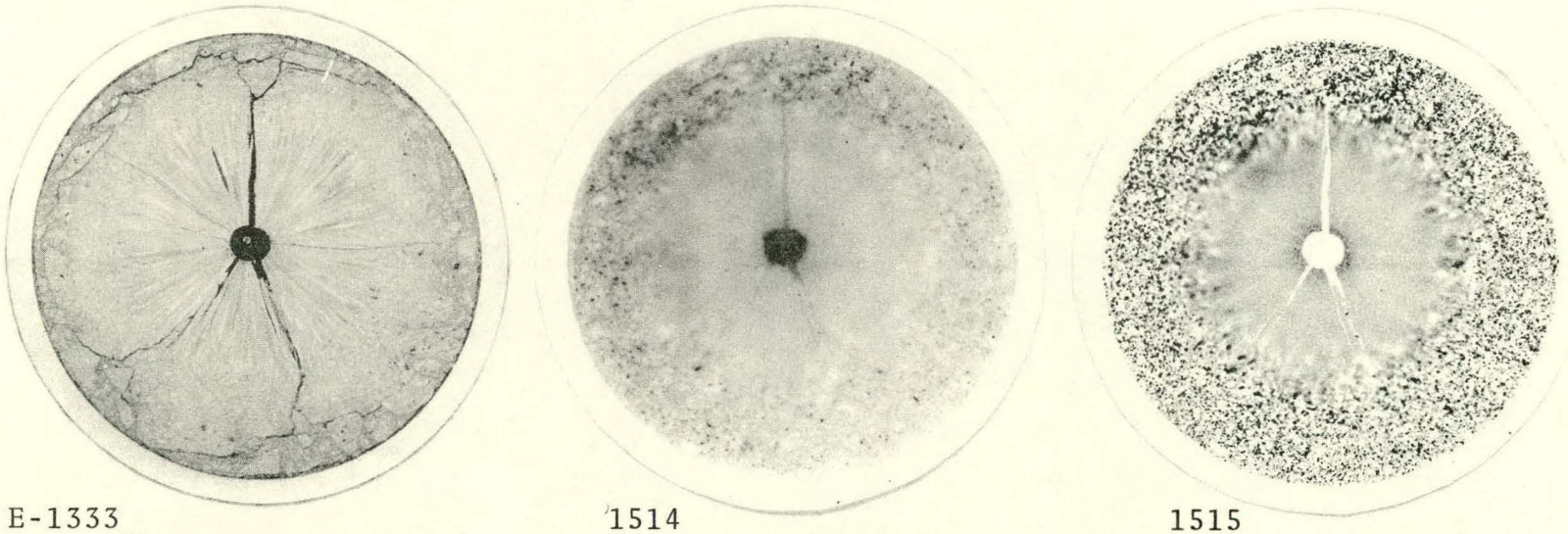

E-1333
Phctomacrograph

1514
β-γ Autoradiograph

1515
α-Autoradiograph

0682721

Transverse Composite

Figure 5

Transverse Section from PRTR Rod FR-62 Containing Pneumatically Impacted, Vibrationally Compacted UO_2-2 wt% PuO_2 fuel. The local power generation was nominally 590 w/cm with maximum fuel temperatures of approximately 2500 °C. Peak burnup of 7800 MWd/MTM.

calculated columnar grain growth boundary if it is assumed that the columnar grain growth temperature is 1800 °C. The beta-gamma and alpha autoradiographs show homogenization of the pneumatically impacted UO_2-PuO_2 fuel mixture to the edge of the columnar grain growth boundary. There is no evidence of fuel melting or significant fission product migration, and maximum fuel temperatures were approximately 2500 °C.

The two other transverse sections examined were from the upper and lower regions of the rod where the estimated power generation was 378 w/cm (11.5 kW/ft). Fuel structures formed during irradiation at the 378 w/cm planes in the upper and lower sections of the rod are similar (Figure 6). No central void or well defined elongated columnar grains formed at either plane although slightly more sintering occurred in the sample examined from the lower section of the rod, i.e., 72% versus 62% of the radius. The difference in sintering radii is within the variation expected for vibrationally compacted fuel; however, the degree of sintering in both samples is considerably greater than expected for a power generation of 378 w/cm under these operating conditions. Based on the observed sintering boundary, calculated temperature isotherms indicate that the apparent in-reactor sintering temperature of the fuel is in the range of 1100-1200 °C, which is considerably lower than expected. Possible reasons for this apparent anomaly are being studied.

A ZrO_2 layer formed on the inner and outer surfaces of the Zircaloy cladding in the peak power region (590 w/cm) of the rod (Figure 7) and the lower power region (378 w/cm) near the bottom end of the rod (Figure 8) with no abnormal hydriding effects. However, the thickness of the ZrO_2 layer on the inner and outer cladding surfaces is greater in the high power region of the rod and is indicative of flux-induced corrosion rates. A maximum ZrO_2 thickness of about 150 mg/dm^2 in the peak flux position is comparable with the growth rates measured on Zircaloy pressure tubes in PRTR. These flux-induced corrosion rates are about a factor of 10 greater than the expected corrosion rate

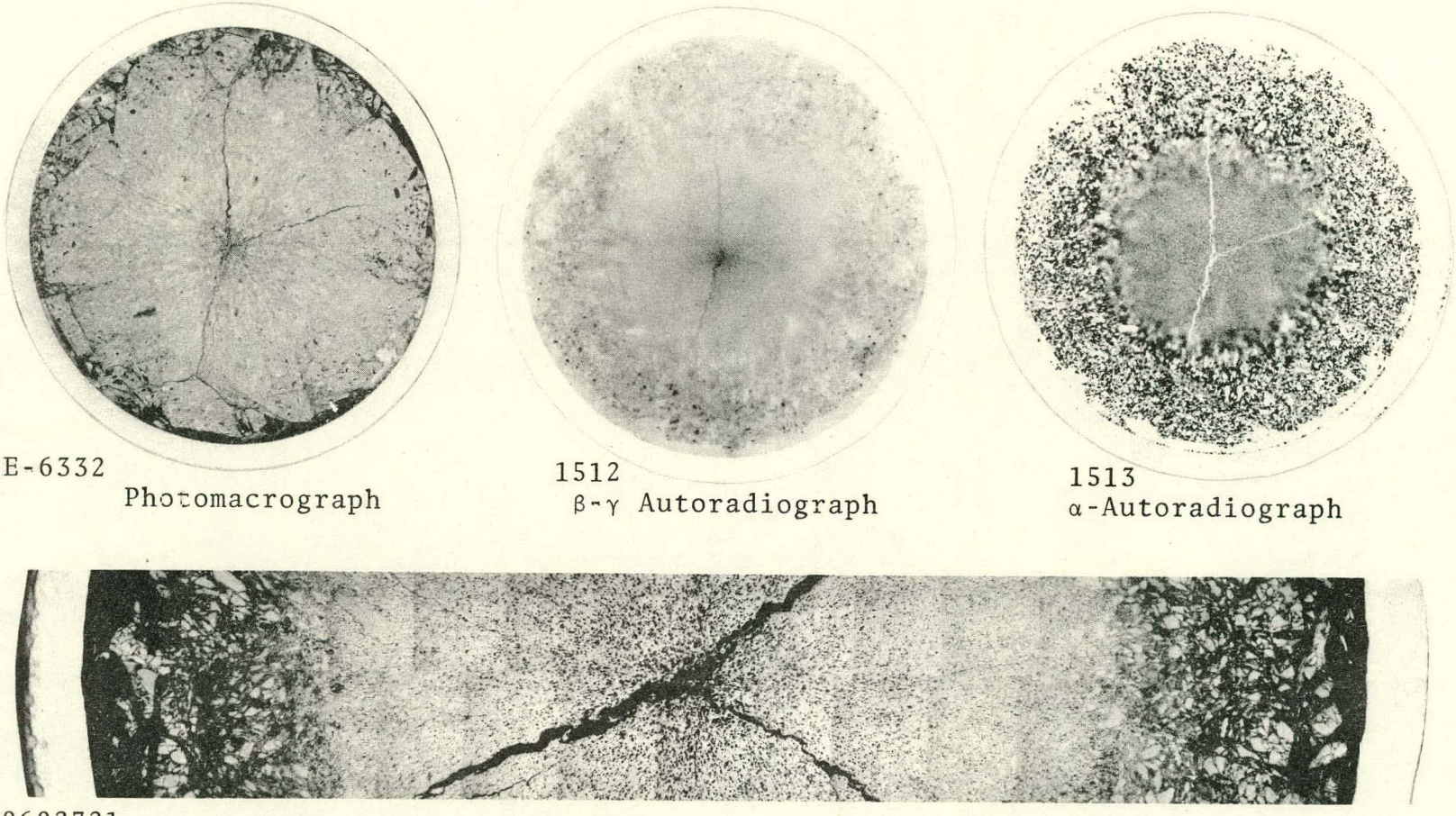

Figure 6

Transverse Section from PRTR Rod FR-62 Containing Pneumatically Impacted, Vibrationally Compacted UO_2-2 wt% PuO_2 fuel. The local power generation was nominally 375 w/cm with maximum fuel temperatures of approximately 1700 °C.

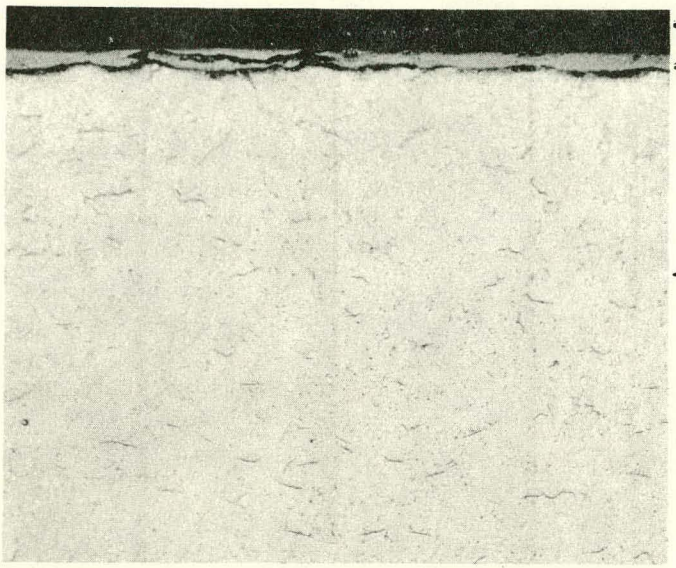

E-6415 250X

(a) Outer Surface

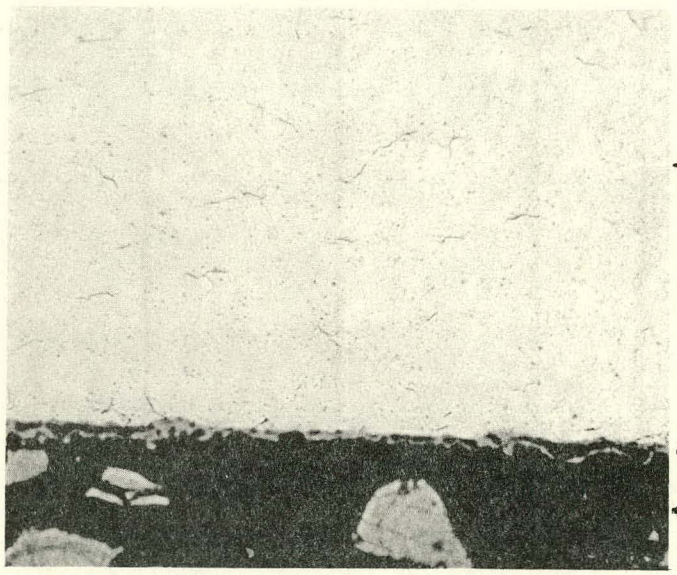

E-6419

(b) Inner Surface

Figure 7

Transverse Metallographic Section of Zircaloy Cladding from the Peak Power (590 w/cm) Position of PRTR Rod FR-62. (Etched)

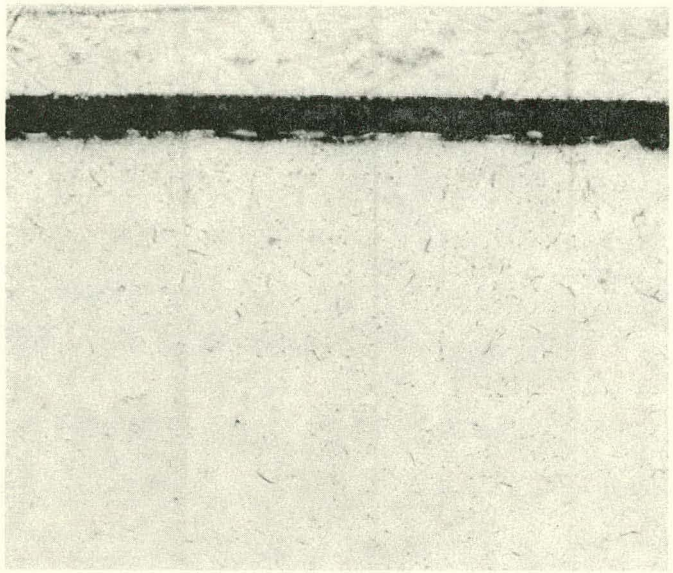

E-6397 250X
(a) Outer Surface

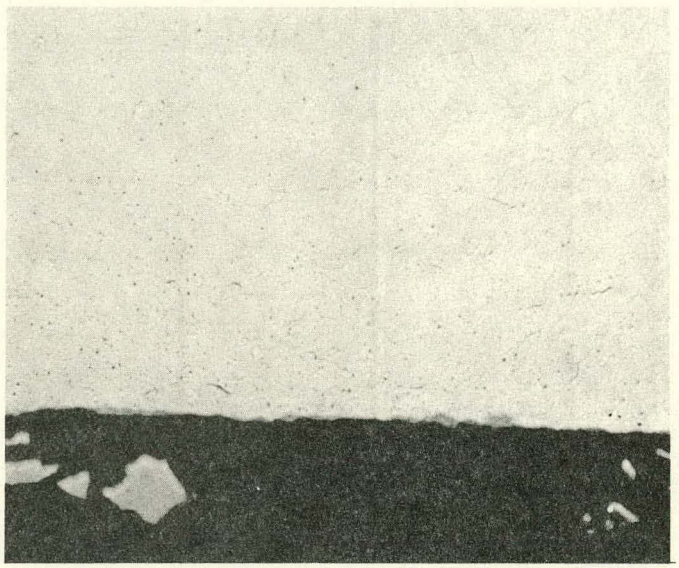

E-6401 250X
(b) Inner Surface

Figure 8

Transverse Metallographic Section of Zircaloy Cladding Near Bottom End (375 w/cm) of PRTR Rod FR-62. (Etched)

for prefilmed Zircaloy exposed to a similar environment in the absence of a neutron flux. Also, the character of the ZrO_2 layer on the inner cladding surface is different in the two locations. The ZrO_2 layer in the peak power region (Figure 7) appears porous and friable, whereas the ZrO_2 layer is dense and more characteristic of what is normally observed in the lower power region (Figure 8). The porous or friable character of the oxide on the inside surface in the peak flux region is attributed to the effects of fission fragment damage due to the close proximity of the fuel material. Similar observations have been reported by other experimenters.

The objective of the fuel testing program in the PRTR Fuel Element Rupture Test Facility (FERTF), a pressurized water loop, is to investigate the effects of specific power and burnup on the defect behavior of pellet and vibrationally compacted fuel rods, and a specially designed 8-rod FERTF test element is being utilized for these experiments. The rod power generation in the FERTF is determined to within approximately ± 3% by flow, differential temperature, and gamma scanning measurements. Relative power generation among rods in the 8-rod FERTF test element is determined by counting the gamma energy peaks associated with $^{95}Zr/^{95}Nb$ with a NaI gamma spectrometer. After allowing cooling periods in excess of two weeks, the minimum cooling time to obtain meaningful results, gamma scanning results show random rod-to-rod power variations of only about ± 1% in nondefected vibrationally compacted rods (Figure 9). This small variation can be attributed to inherent differences in the vibrationally compacted rods and statistical variations in gamma scanning.

Fuel rods irradiated in the FERTF have been destructively examined to relate fuel structures formed with power generation. Temperatures normally associated with observed structural features in the fuel, e.g., columnar grain growth radius and the diameter of the sintering boundary, are used to estimate temperature conditions of the fuel during irradiation. With a couple of exceptions, there is reasonably good agreement between the

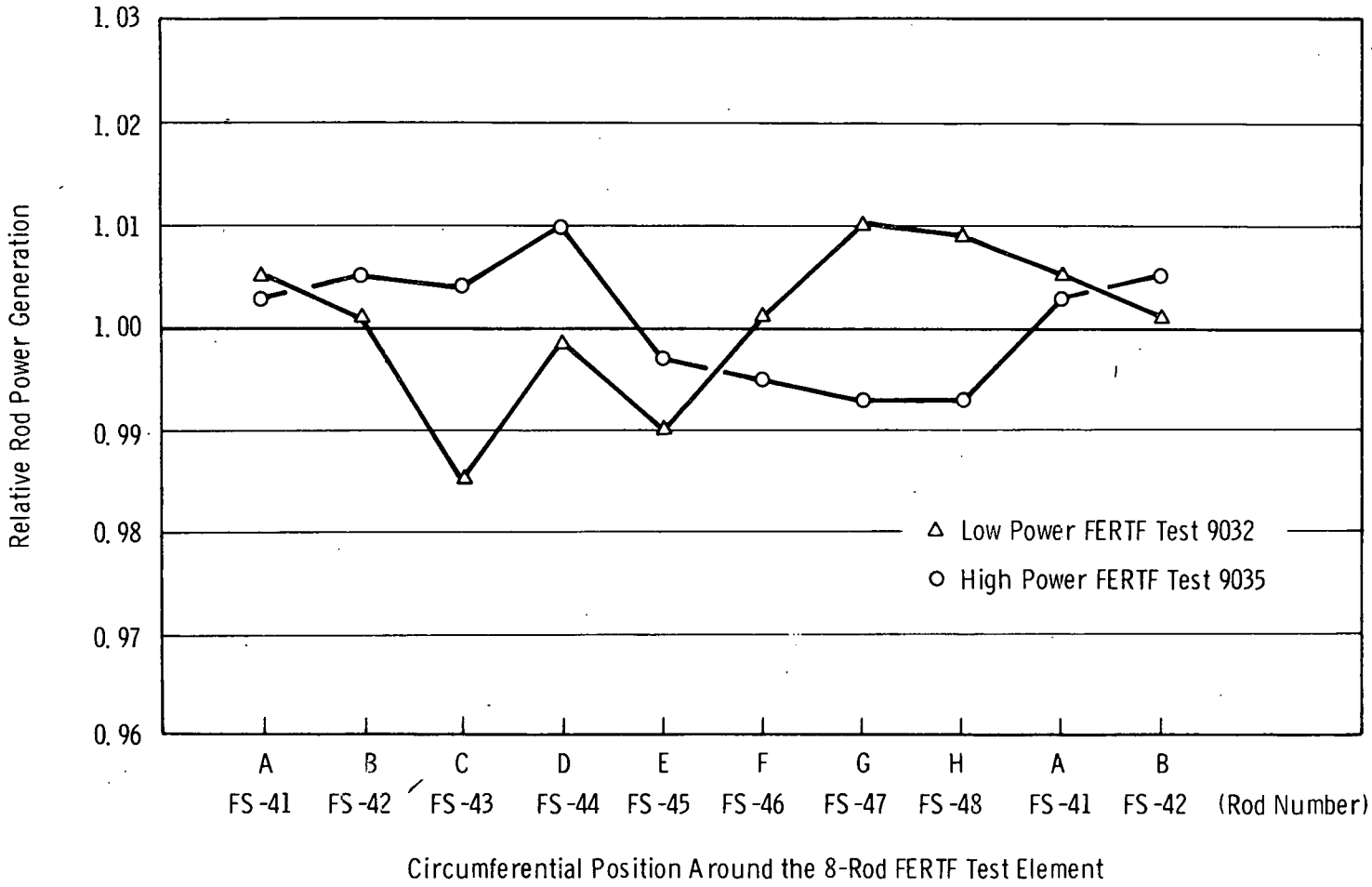

FIGURE 9 Relative Power Generation Among the Eight Rods in the FERTF Test Element for the Low Power Test 9032 and the High Power Test 9035.

calculated and experimentally indicated temperature conditions. The data indicate that the columnar grain growth and sintering radii formed during irradiation are within ± 5% of the calculated values if it is assumed that the columnar grain growth and sintering temperatures are 1800 and 1700 ^{o}C, respectively (Figures 10 and 11). This variation is indicative of inherent rod-to-rod behavioral differences in vibrationally compacted fuel.

When using either the columnar grain growth or sintering boundary as indicators, variations in deduced operating conditions are within ± 5%; however, the sintering boundary appears to provide more consistent results. For instance, in one set of three rods irradiated under the same power generating conditions (590 w/cm) and exposed to the identical power history during 10 days of irradiation, columnar grain growth and center void formation occurred in two rods whereas a significantly lower temperature condition was indicated in the third rod by the absence of columnar grains and a center void (Figure 12). Well defined lenticular voids were present in the fuel in one of the rods in which there were significantly different structural features in "pie-shaped" segments of the cross section. Such rod-to-rod structural differences and local structural variations within the fuel tend to disappear with increasing exposure. In spite of these differences or apparent anomalies, however, the sintering boundary radii for the three rods were within ± 5%.

Fission Product Migration

Gamma scanning of irradiated, vibrationally compacted UO_2-PuO_2 fuel rods after short cooling periods has indicated localized high activity regions over short axial distances (Figure 13). Postirradiation examination of one of the rods in a region that indicated a localized activity increase as much as 14% above average did not reveal any structural variations in the fuel indicative of a localized high power generation area or "hot spot"; however, transverse cracks containing high fission product activity were present in the fuel in the region of high activity indicated by gamma scanning (Figure 13). Gamma energy spectra show that the high activity regions contain high concentrations

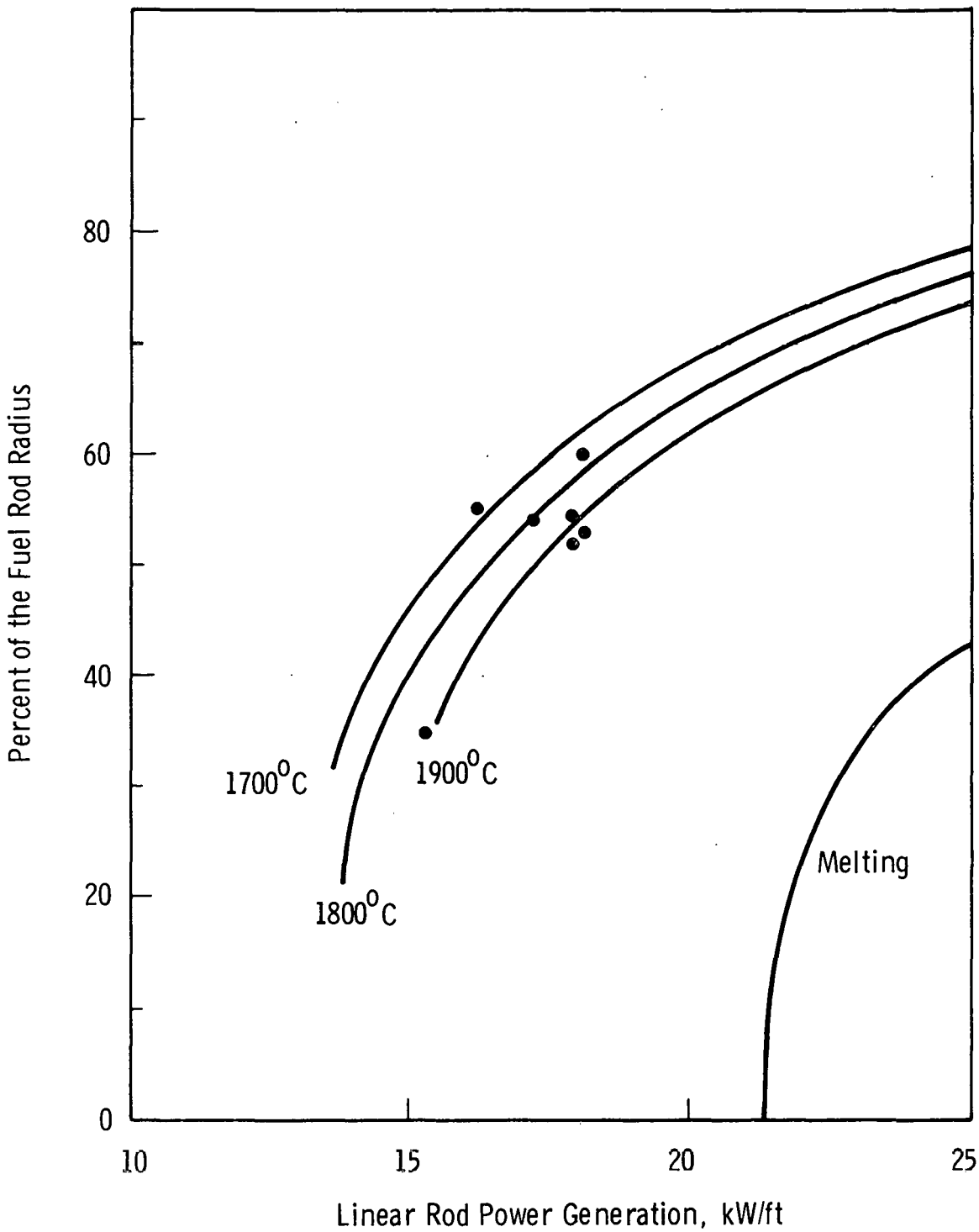

FIGURE 10. Calculated Temperature Isotherms in a Vibrationally Compacted UO_2-2 wt% PuO_2 PRTR Fuel Rod and Experimentally Determined Columnar Grain Growth Radii.

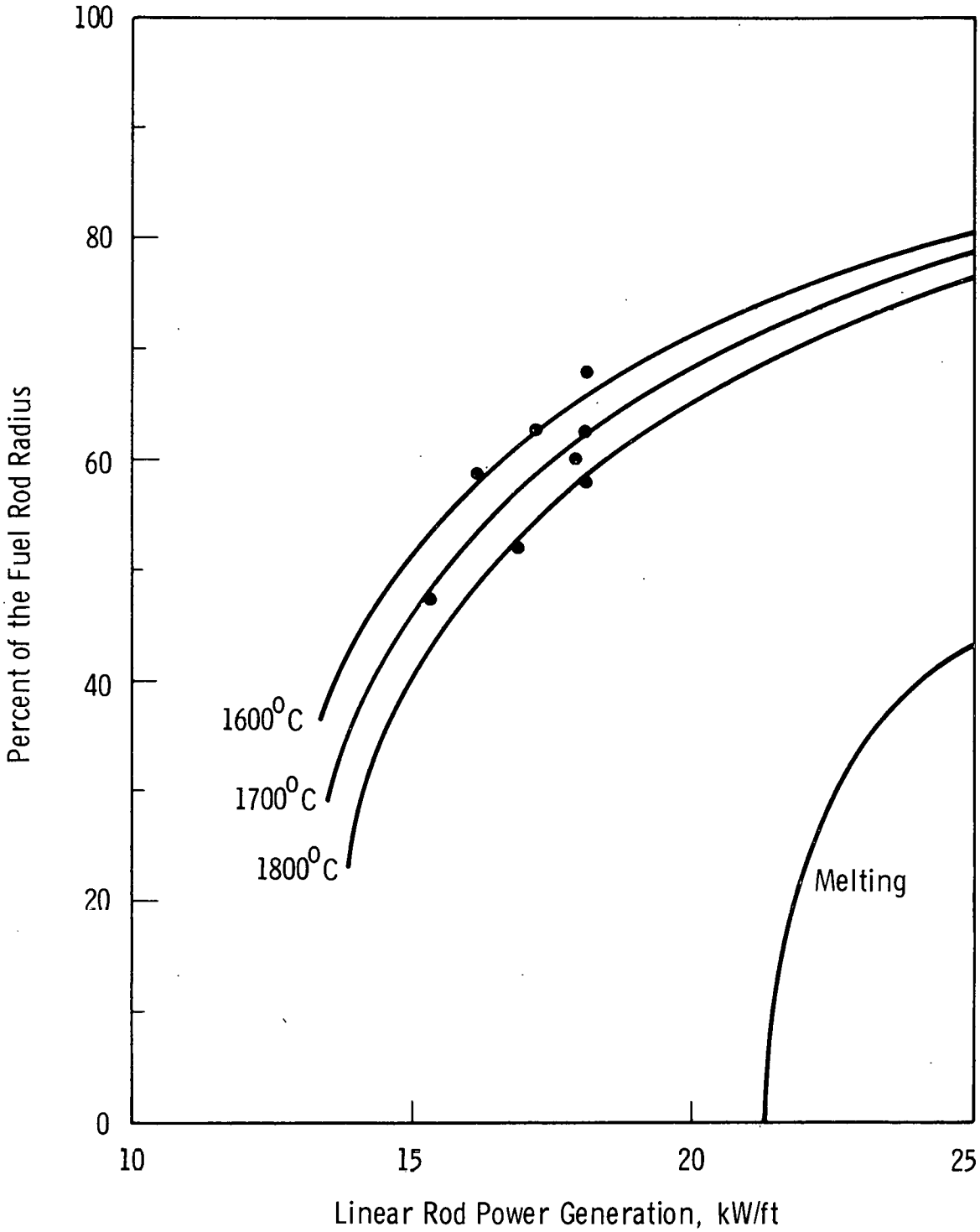

FIGURE 11. Calculated Temperature Isotherms in a Vibrationally Compacted UO_2-2 wt% PuO_2 PRTR Fuel Rod and Experimentally Determined Sintering Boundary Radii.

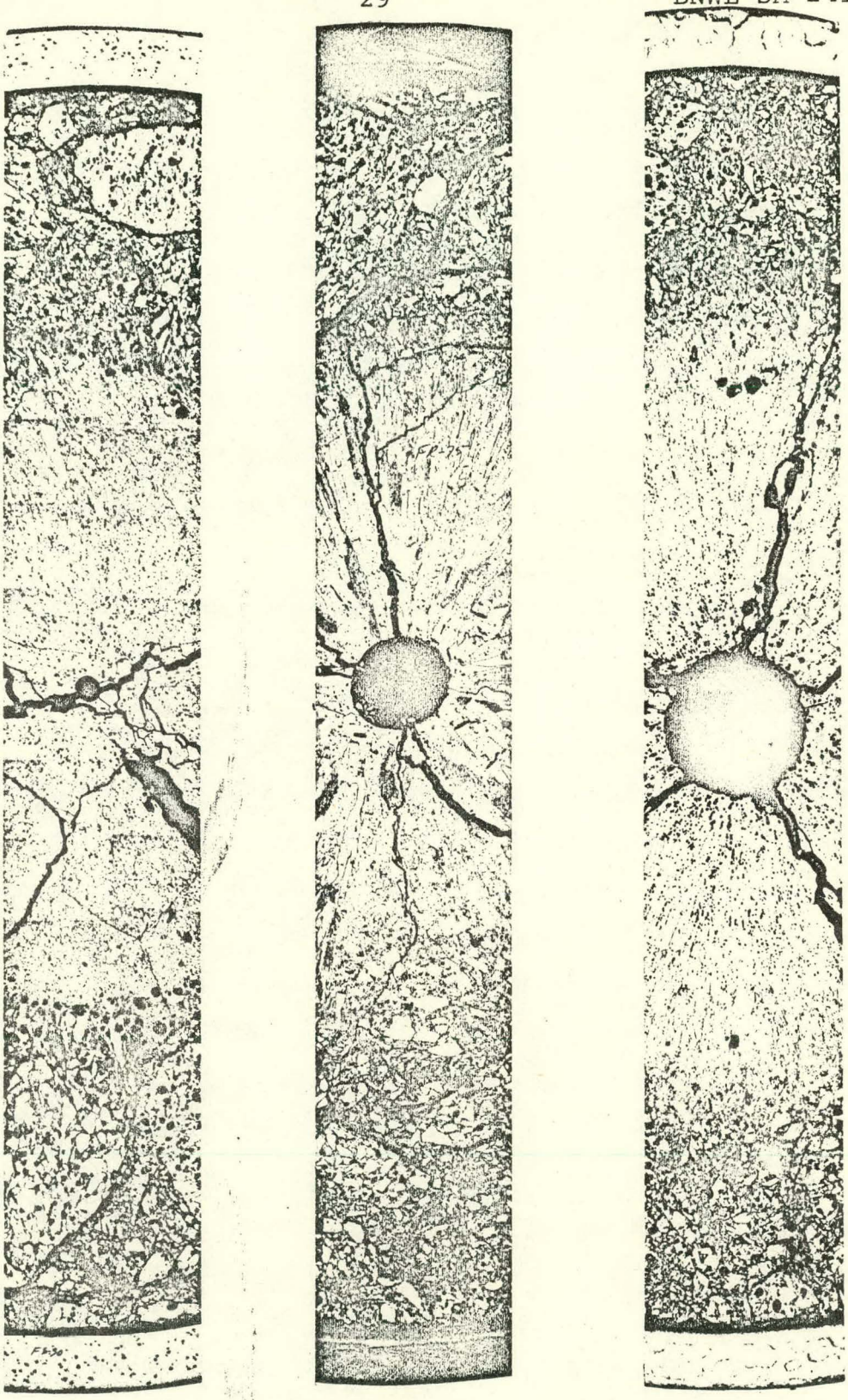

Rod FS-30 Rod FR-75 Rod FR-28

Figure 12. Transverse Composite of Three Vibrationally Compacted UO_2-2 wt% PuO_2 Fuel Rods Irradiated Under Identical Conditions in the FERTF. Significantly different structural features formed at a peak power of 583 ± 7 w/cm (17.8 ± 0.2 kW/ft).

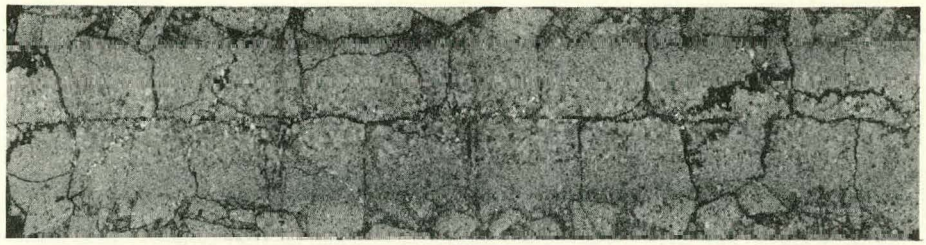

Photomacrograph

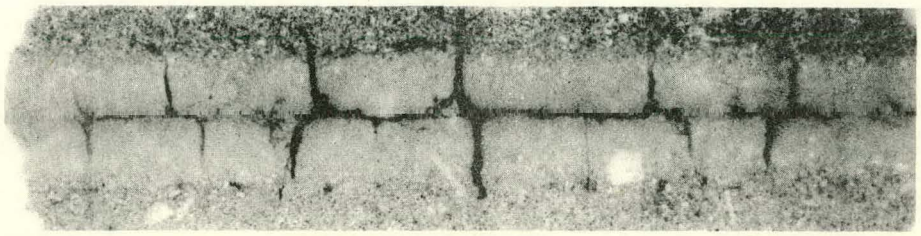

β-γ Autoradiograph

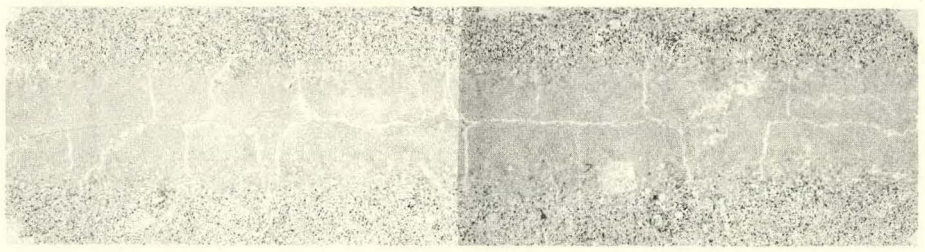

α Autoradiograph

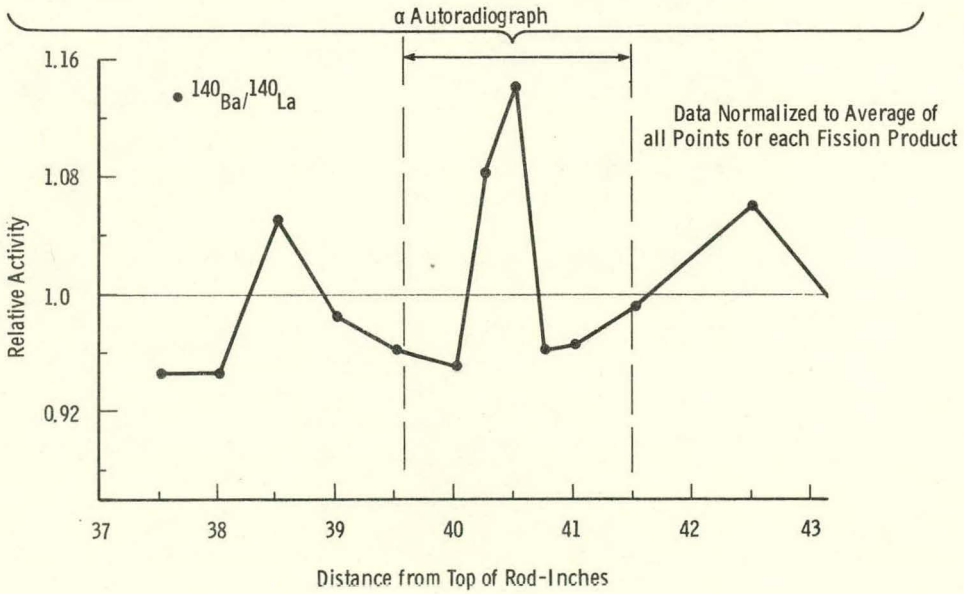

Figure 13. Longitudinal Section Through a Vibrationally Compacted UO_2-2 wt% PuO_2 Fuel Rod (FS-30). The high activity cracks in the fuel correspond with the localized high activity region indicated by gamma scanning.

of what is most likely 12.8-day $^{140}Ba/^{140}La$. Thermodynamic considerations predict the migration of barium.

Recent observations made during postirradiation examinations have indicated what may be a more sensitive indicator of fuel operating conditions than the extent of the columnar grain growth or sintering boundary radii. Beta-gamma autoradiographs of transverse UO_2-PuO_2 fuel specimens taken relatively soon after discharge from the reactor have shown high fission product concentrations located at the outer sintering boundary (Figure 14). This deposition, which tends to concentrate in circumferential cracks, is in addition to the normal fission product distribution patterns. The high activity is presumed to be caused primarily by 12.8-day ^{140}Ba which has diffused down the thermal gradient.

Decay of the activity is illustrated by the beta-gamma autoradiographs taken at different times after shutdown. The high fission product activity regions may be related to the grey phase observed in the equiaxed grain region of high burnup UO_2-PuO_2 fuel[21]. Barium has been identified as the most abundant fission product in the grey phase with cerium and strontium concentrations estimated to be less than 10%[21]. The location of this fission product in the fuel should be highly dependent upon the local fuel temperature, hence, a sensitive indicator of fuel operating conditions.

Fission Gas Release

The amount of fission gas release has been determined for full-sized vibrationally compacted PRTR fuel rods containing pneumatically impacted UO_2-PuO_2 fuel[22]. A plot of percent

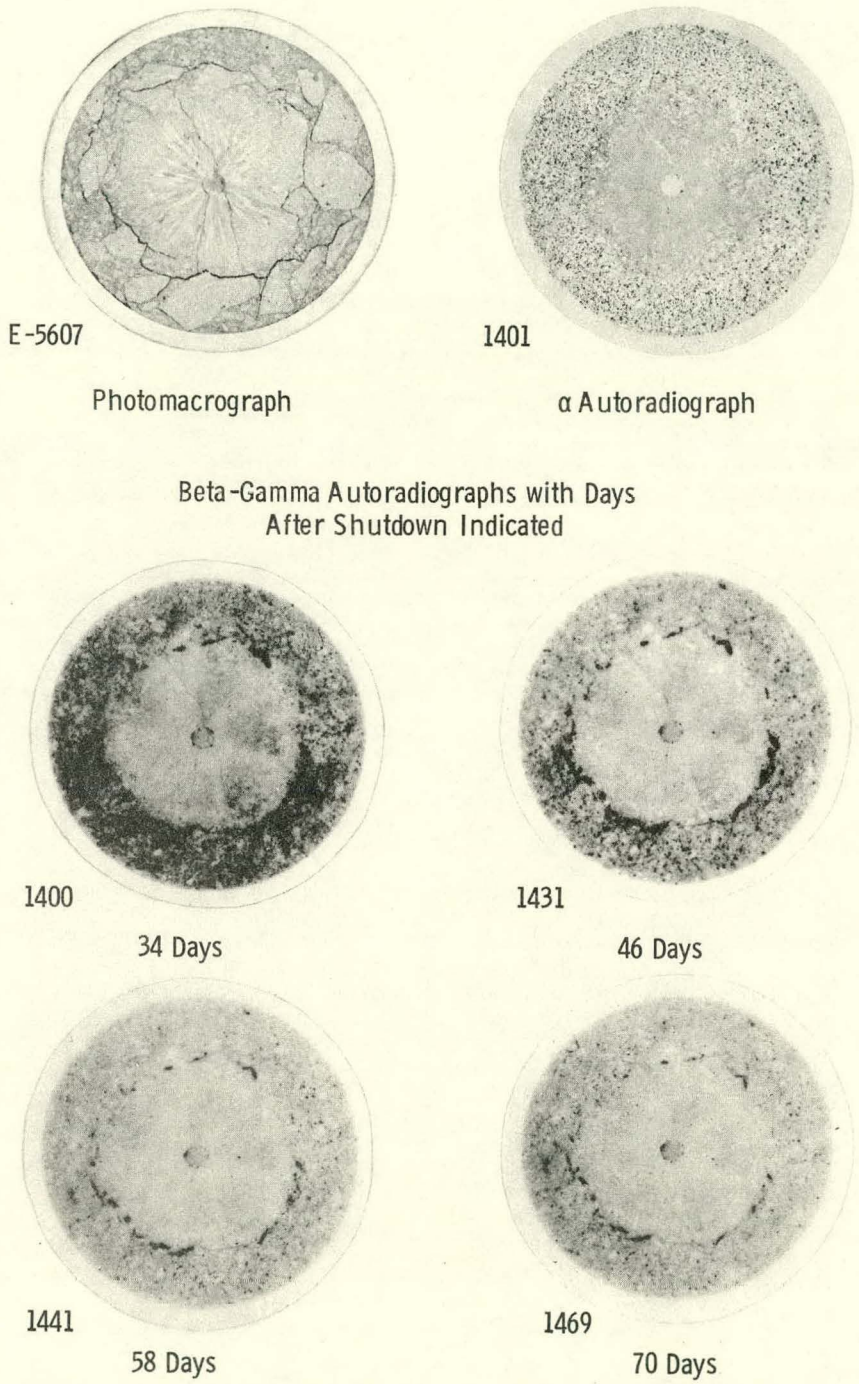

Figure 14. Transverse Section of a Vibrationally Compacted UO_2-PuO_2 PRTR Fuel Rod With High Fission Product Activity Located at the Outer Sintering Boundary. Decay of the Activity, Presumed to be Caused by 12.8 day ^{140}Ba, is Illustrated by the β-γ Autoradiographs Taken at Different Times After Shutdown.

Xe + Kr release versus volumetric average fuel rod temperature $\bar{T}_v$ * for fuel rods with burnups ranging from 100 to 5000 MWd/MTM is given in Figure 15. The results show a maximum of 92% Xe + Kr release from fuel rods that operated with volumetric average fuel rod temperatures of about 2200 °C produced at a maximum rod power of 890 w/cm in PRTR. Based upon comparable volumetric average fuel temperatures, the data also indicate that the fission gas release fraction for vibrationally compacted and pellet-containing fuels is comparable. Fission gas release values are expected to increase with increasing burnup, particularly for the low fractional release values. However, the high fractional release values should not change appreciably with irradiation time because the rate of gas release from the high temperature fuel is more rapid. Different rods from the same element, sampled in either the fuel or plenum region, yielded approximately the same quantity of gas, which indicates good communication along the entire length of the fuel rods and between plenum and fuel.

---

*Volumetric average fuel temperatures are based on calculated temperature profiles within the fuel by using an estimated thermal conductivity of packed particle UO_2 as a function of temperature and the indicated thermal conductivity of UO_2 at 2800 °C as the thermal conductivity of molten fuel. The flux depression within UO_2-PuO_2 fuel rods is calculated with the THERMOS computer code. The volumetric average fuel temperature over the entire volume of the fuel rod is defined as:

$$\bar{T}_v = \frac{Tv}{\phi/\bar{\phi}}$$

where: $\bar{T}_v$ = Volumetric average fuel temperature within the fuel rod

T_v = Calculated area weighted average fuel temperature at the maximum flux position

ϕ = Peak neutron flux

$\bar{\phi}$ = Average neutron flux along the length of the fuel rod.

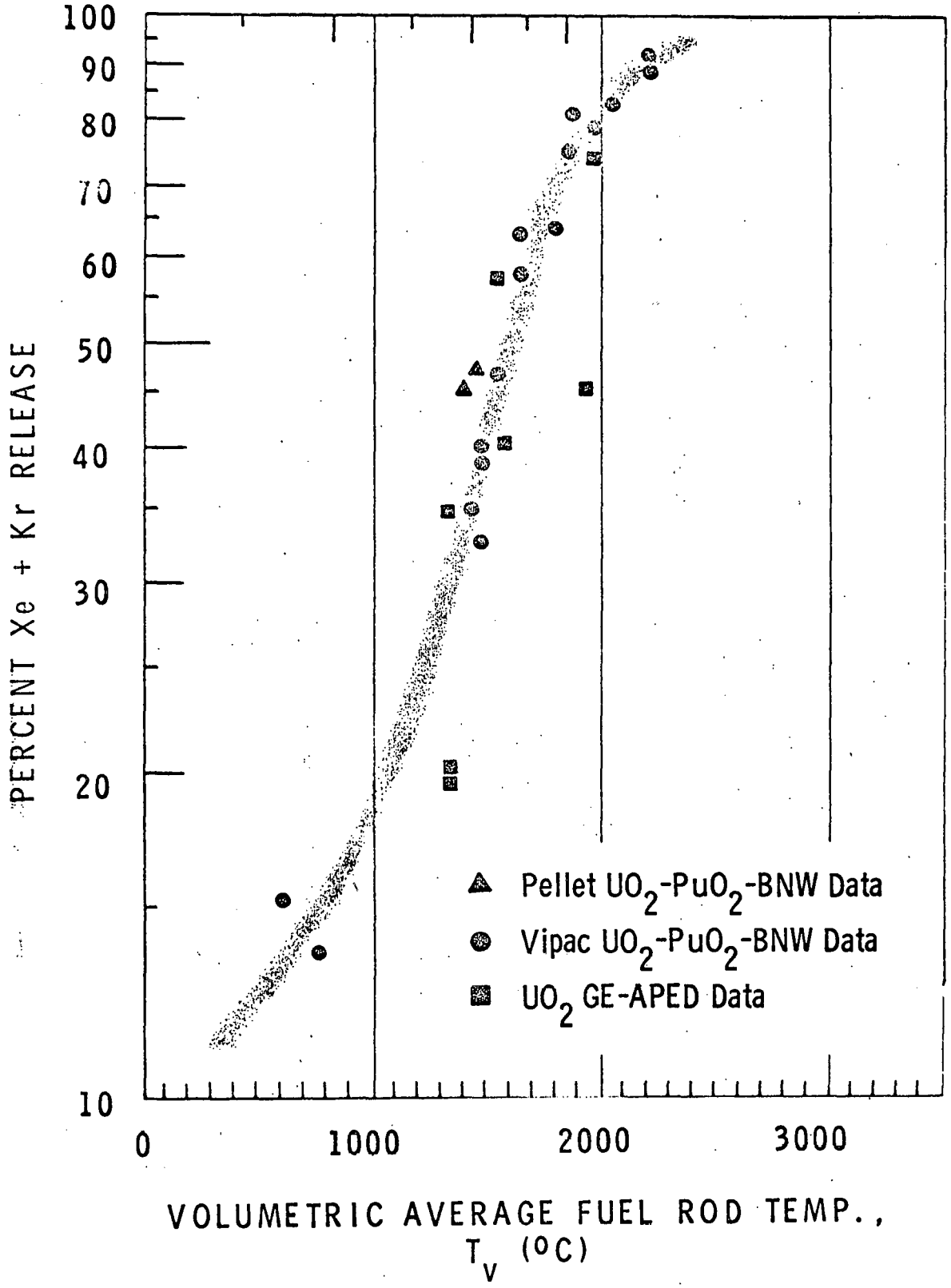

Figure 15. Fission Gas Release as a Function of Volumetric Average Fuel Rod Temperature in Vibrationally Compacted UO_2-PuO_2 PRTR Fuel Rods.

Fission gas release values can be calculated with reasonable accuracy if it is assumed that 100% of the gas is released from the fuel volume operating above 1800 °C (columnar grain growth region) and if 10% is released from the fuel operating below 1800 °C[22]. These data were calculated from capsule irradiation tests and agree well with the gas release values obtained with the long fuel rods irradiated in PRTR.

Comparison of the gas release data obtained from vibrationally compacted, pneumatically impacted UO_2-PuO_2 fuel with that derived in earlier work using coprecipitated and sintered fuels suggests possible lower fission gas release values for pneumatically impacted material[23]. However, the comparison is difficult because of differences in specimen characteristics, particularly density, and more definitive data are needed before meaningful conclusions can be drawn.

In a carefully controlled experiment, Carroll and Sisman[24] of Oak Ridge National Laboratory compared the fission gas release characteristics of pneumatically impacted UO_2 with those of arc-fused single crystal UO_2. A considerable difference exists in these two gas release rates: the single crystal UO_2 release rate at 1000 °C is an order of magnitude greater and increases with temperature faster than the release rate from the pneumatically impacted material. Carroll and Sisman[24] postulate "that grain boundaries do not act as paths of rapid escape, as once believed, but rather as traps which anchor migrating fission gas." The polycrystalline structure of pneumatically impacted fuel material could explain its lower gas release at moderate temperatures. However, at temperatures resulting in sintering and grain growth, the gas release characteristics of the two fuel materials should be nearly the same.

Instrumented experiments are being conducted in PRTR to determine the effects of rod power and burnup on gas release and pressure buildup in vibrationally compacted mixed-oxide fuel rods during irradiation[25]. Two of the four instrumented

fuel rods have operated at peak rod powers of 310 w/cm to peak burnups of 6000 MWd/MTM (Figure 16). The internal pressure in these fuel rods increased with burnup at a nearly constant rate to a burnup of 3700 MWd/MTM, at which time the fuel operating conditions were increased from a peak power rating of nominally 295 w/cm to 360 w/cm. This change resulted in an increase in the estimated volumetric-averaged fuel temperature from 750 to 940 ^{o}C. The rate of pressure increase changed at this point to a higher, but still nearly constant rate. There is good agreement between actual and calculated pressure buildup rates which correspond to 13% release of the fission gases formed, even though the absolute pressure due to sorbed gases and moisture release, i.e., the internal pressure at zero burnup, is considerably less than expected.

The other two instrumented fuel rods have operated at peak power of 560 w/cm with maximum fuel temperatures of approximately 2500 ^{o}C to peak burnups of 9900 MWd/MTM (Figure 17). These rods operated with the onset of fuel melting for a short period of time (about 8 hrs) during the early part of their irradiation. The internal pressure increased at nearly a constant rate with burnup, with most of the fission gas release occurring in a stepwise manner during shutdown-startup power cycles, and no significant changes in pressure were observed during steady-state operation. The experimentally determined rate of pressure buildup is in good agreement with the calculated rate and corresponds to 25 percent release of the fission gases formed. Even though the rate of pressure buildup in the high power fuel rods has been as predicted from gas release data, the absolute internal pressure within the rods is considerably less than expected. Analysis and interpretation of the data indicate that, within the burnup and fuel temperature ranges tested:

1. Internal pressure due to the release of sorbed gases and moisture from the fuel is considerably less than predicted if 100% release of the

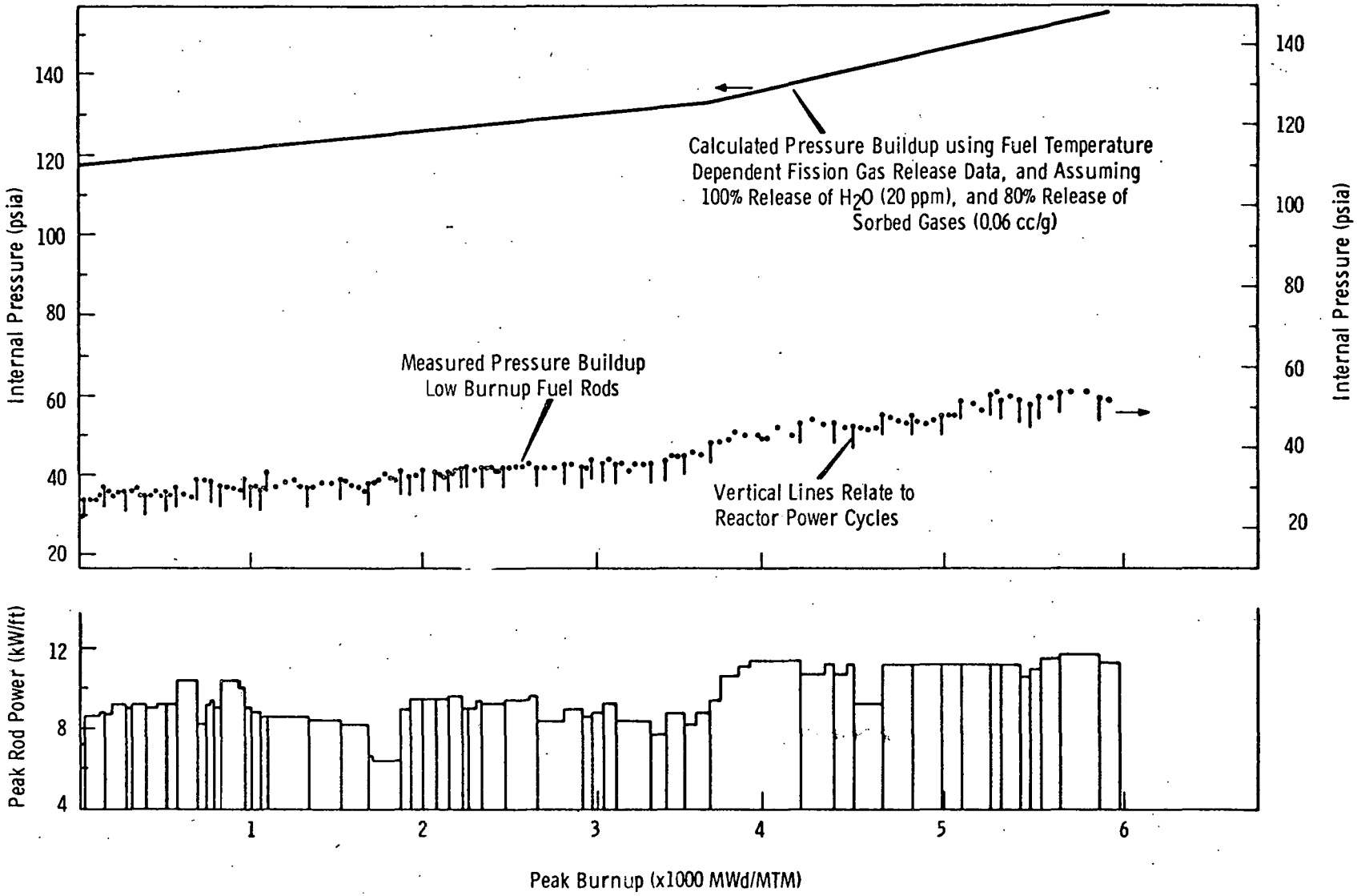

FIGURE 16 . Internal Pressure Buildup in Low Power UO_2-PuO_2 PRTR Fuel Rods.

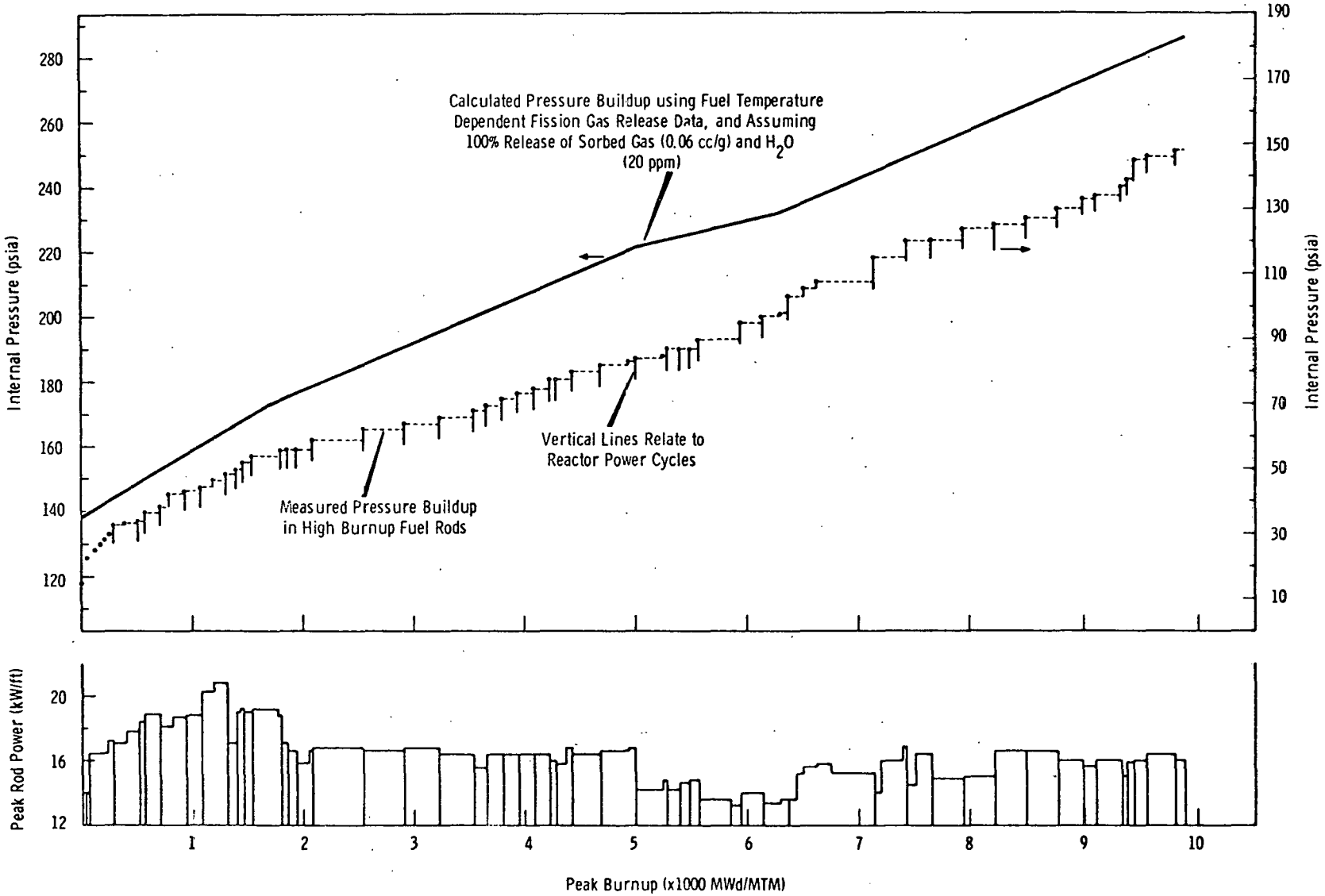

FIGURE 17. Internal Pressure Buildup in High Power UO_2-PuO_2 PRTR Fuel Rods.

analytically determined amounts is assumed. Based upon the known amounts of sorbed gases and moisture present in the fuel and the volumetric average fuel temperature, the predicted release of these constituents should have resulted in a considerably higher internal gas pressure during the initial fuel heatup. It is suspected that most of the entrapped oxygen and moisture are released from the fuel during the initial stages of irradiation and react rapidly with the unautoclaved Zircaloy cladding to form an oxide layer on the inner surface and some of the hydrogen is absorbed. Some of the oxygen may also react with the lower temperature fuel material.

2. Internal pressure buildup rates are consistent with fission gas release fractions predicted from measurements made previously on similar PRTR fuel. The previous study related fission gas release fractions to volumetric-averaged fuel temperatures (Figure 15).

3. Internal gas pressure increases in a stepwise manner during reactor power cycles (shutdown-startup periods) and levels off during steady power operation in the high power rods; however, the stepwise pressure increases in the low pressure rods are comparatively small and, in most cases, are not detectable. This behavior suggests a different predominance of the contributing gas release mechanisms in the high and low power rods

   It is hypothesized that in the high power rods, fission gas mobility is a diffusion controlled mechanism in which the gas release is retarded during short steady-state operating periods by

trapping sites within the fuel. Release takes place primarily when thermal stress-induced cracking occurs during power cycling. This hypothesis is supported by the fact that the magnitude of the stepwise increases is related to the length of the steady-state operating period immediately preceding the power cycle.

Diffusion controlled fission gas mobility is less pronounced in the low power rods, and a recoil-knckout process is probably the predominant release mechanism. This mechanism results in a more continuous release of gaseous fission products during steady-state operation, and stepwise increases are less predominant.

4. The rate of pressure buildup due to fission gas release is independent of burnup or burnup rate to the levels achieved thus far in the experiment (9900 MWd/MTM peak).

5. Average plenum gas temperatures vary directly with, and are slightly higher than maximum coolant temperatures. Fuel temperature has an insignificant effect on plenum gas temperature.

The irradiation of these instrumented experiments will continue to peak burnups of approximately 45,000 MWd/MTM.

VI. Defect Behavior

The postulated catastrophic defect behavior of ceramic packed particle fuels, and in particular vibrationally compacted fuels, has not materialized[26]. In general, the defect behavior of packed particle fuel operating at heat ratings currently employed in power reactors has been satisfactory. These results have been corroborated by in-service fuel defect experience and intentionally defected experiments which included single rod tests, prototype elements, and full-size PRTR fuel elements tested over a wide

range of conditions. In-reactor sintering undoubtedly improves the washout characteristics of the vibrationally compacted fuel rods. Based upon a limited amount of experience at the higher power generations, there is some evidence which indicates that the defect behavior mode may change in the range of 800 to 900 w/cm and could become the limiting criterion for advanced or very high power operation.

Intentionally Defected Experiments

Irradiation testing of deliberately defected fuel rods is performed in the Fuel Element Rupture Test Facility (FERTF) in PRTR and in a pressurized water loop in the Engineering Test Reactor (ETR) using full-size PRTR fuel elements, prototype elements, and single rods. The types of defects studied have included 1.5 mm diameter holes and slits up to 170 mm long. Peak rod power generations in pre-irradiated and nonirradiated intentionally defected experiments were in the range of 200 to 890 w/cm with a considerable portion of the fuel molten at the higher powers (Figure 18). A summary of the packed particle element defect tests performed in the FERTF is presented in Table III[26].

Release characteristics for the different types of defects studied are determined by analyzing the ratios of nuclides released to the coolant. Generally, the defect behavior of ceramic packed particle elements has been excellent. No appreciable fuel washout, fuel rod deformation, water-logging effects, or excessive hydriding of the Zircaloy cladding was observed in any of the packed particle fuel element defect tests. The only exception was the rupture of a deliberately defected UO_2-PuO_2 rod operating with considerable fuel melting at the plane of the defect[27]. There was evidence of fuel oxidation and an unexpected large amount of fuel melting in the ruptured rod which may have been the underlying cause of failure. Excessive melting could have been caused by a decrease in the effective thermal conductivity of the fuel, a decrease in the

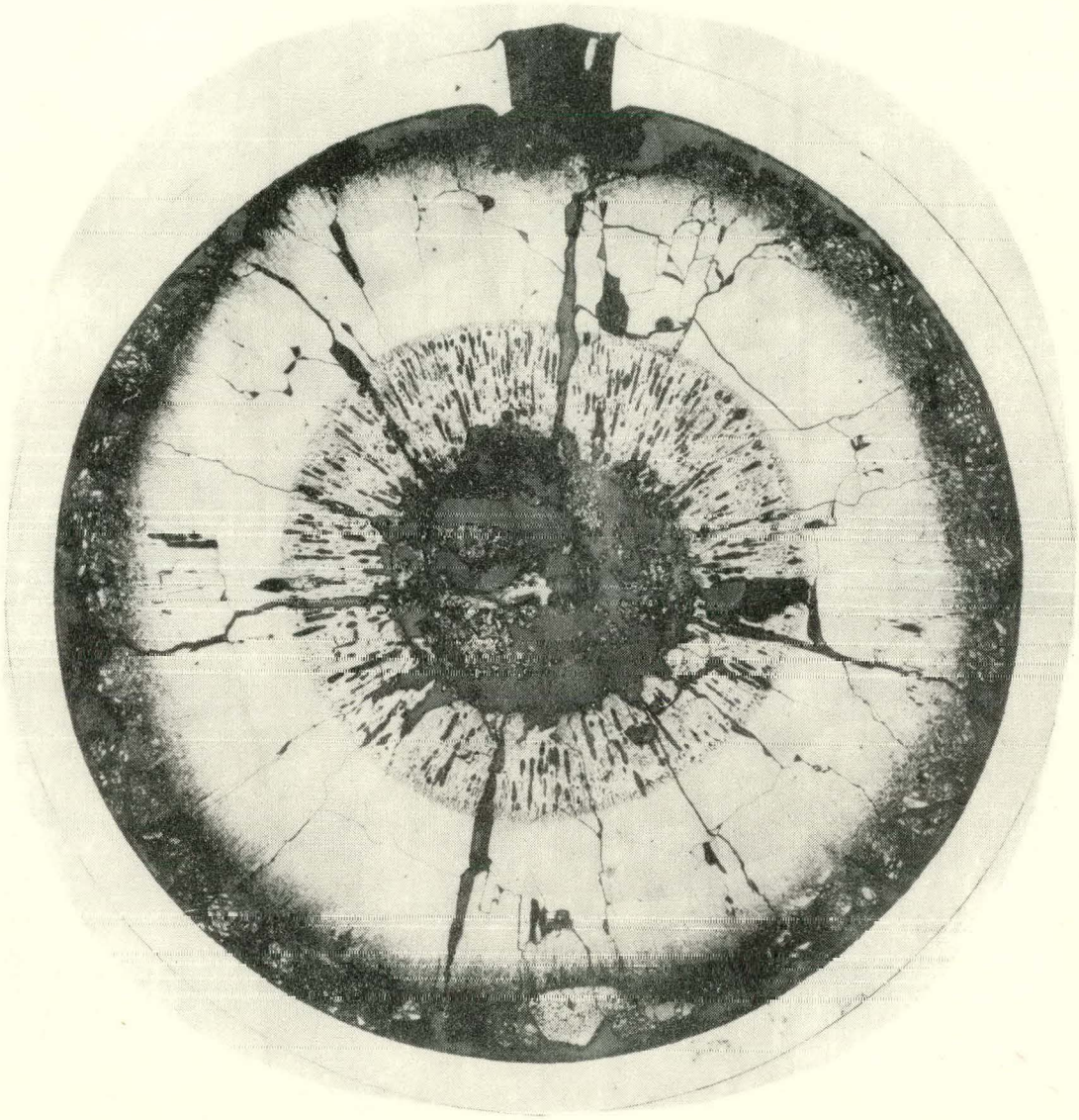

Figure 18. Photomosaic of a Transverse Section Through an Intentionally Defected Vibrationally Compacted UO_2-2 wt% PuO_2 PRTR Fuel Rod. Rod power was 790 w/cm with fuel melting to ~50% of the radius.

TABLE III

Coolant Activities from Defected Packed Particle PRTR Elements Irradiated in the FERTF

Test No.	Element Type and No.	Cladding Defect	Maximun Rod Power w/cm	Irradiation Time, days	Loop Activity, (cpm) Steady State GM (β,γ)	DN (delayed neutron)	Burst Activity GM (β,γ)	Type of Release
A.	Swaged UO_2 FE-1069	1.5 mm diam hole	240	∿ 17	8,000	4,000	220,000	Leaker (a)
B.	Swaged UO_2 FE-1039	16 mm long longitudinal slit	230	∿ 4	23,000 (b)	13,000 (b)	700,000	--
C.	Swaged UO_2 FE-1039	80 mm long longitudinal slit	230	+∿ 19	23,000	13,000	100,000	Diffusion (c
D.	Swaged UO_2 FE-1030	170 mm long longitudinal slit	200	∿ 16	68,000	38,000	150,000	Diffusion
E.	Vibrationally Compacted UO_2 FE-1067	75 mm long longitudinal slit	240	∿ 22	47,000	26,000	170,000	Diffusion
F.	Vibrationally Compacted UO_2 FE-1067	100 mm long longitudinal slit	240	+∿ 8	60,000	31,000	--	Diffusion
G.	Vibrationally Compacted UO_2-2 wt% PuO_2 Fe-6004	1.5 mm diam hole	790	∿ 2.5	80,000	4,000	660,000	Leaker
H.	Vibrationally Compacted UO_2-4 wt% PuO_2 FE-6504	1.5 mm diam hole	890	< 1	7.7×10^6 (b)	1.6×10^5 (b)	--	(Ruptured)

(a) Poor communication between fuel and coolant - long delay time.
(b) Test was discontinued before stable form of release was established.
(c) Good communication between fuel and coolant - short delay time.

melting temperature, a higher than expected power generation due to venting of the fission gas poisons through the defect, or a combination of these effects.

A defect test of a prototype element in ETR provides a dramatic demonstration of the satisfactory defect behavior of vibrationally compacted fuel under extreme operating conditions. In this experiment one rod of a seven-rod cluster containing vibrationally compacted UO_2 fuel was defected with a 1.5 mm diameter hole. The fuel rod operated at 890 W/cm with as much as 60% of the fuel radius molton with very little fuel washout and no clad distortion occurring (Figure 19). This fuel operated for nine effective full power days and was subjected to three programmed reactor shutdowns and startups and one scram recovery startup. During the scram recovery, power was increased from 0 to 50% of full power in less than 3 minutes. In spite of this sudden power increase there was no excessive fuel washout. The release of gaseous fission products to the coolant sharply increased during the scram recovery but soon returned to the release rate normally obtained during steady-state operation.

PRTR In-Service Defects

Thirty-seven in-service defects of packed particle oxide fuel rods have occurred in PRTR without causing serious operating problems. These include 1 swage compacted UO_2 rod out of 1254 irradiated, 20 swage compacted UO_2-PuO_2 rods out of 1824 irradiated, and 16 vibrationally compacted UO_2-PuO_2 rods out of 2242 irradiated. To place these defects in proper perspective in the overall evaluation of packed particle fuel performance, it is important to realize that all but two of the defects are attributed to impurities in the fuel material and not to inherent problems associated with the packed particle process, per se.

The defects attributed to impurities in the fuel material occurred over a relatively short period of time and were caused by (1) fluoride contamination in the plutonium, (2) sorbed moisture on the oxide fuel particles, and (3) traces of hydrocarbons in the form of oil inadvertently introduced by the failure of mechanical

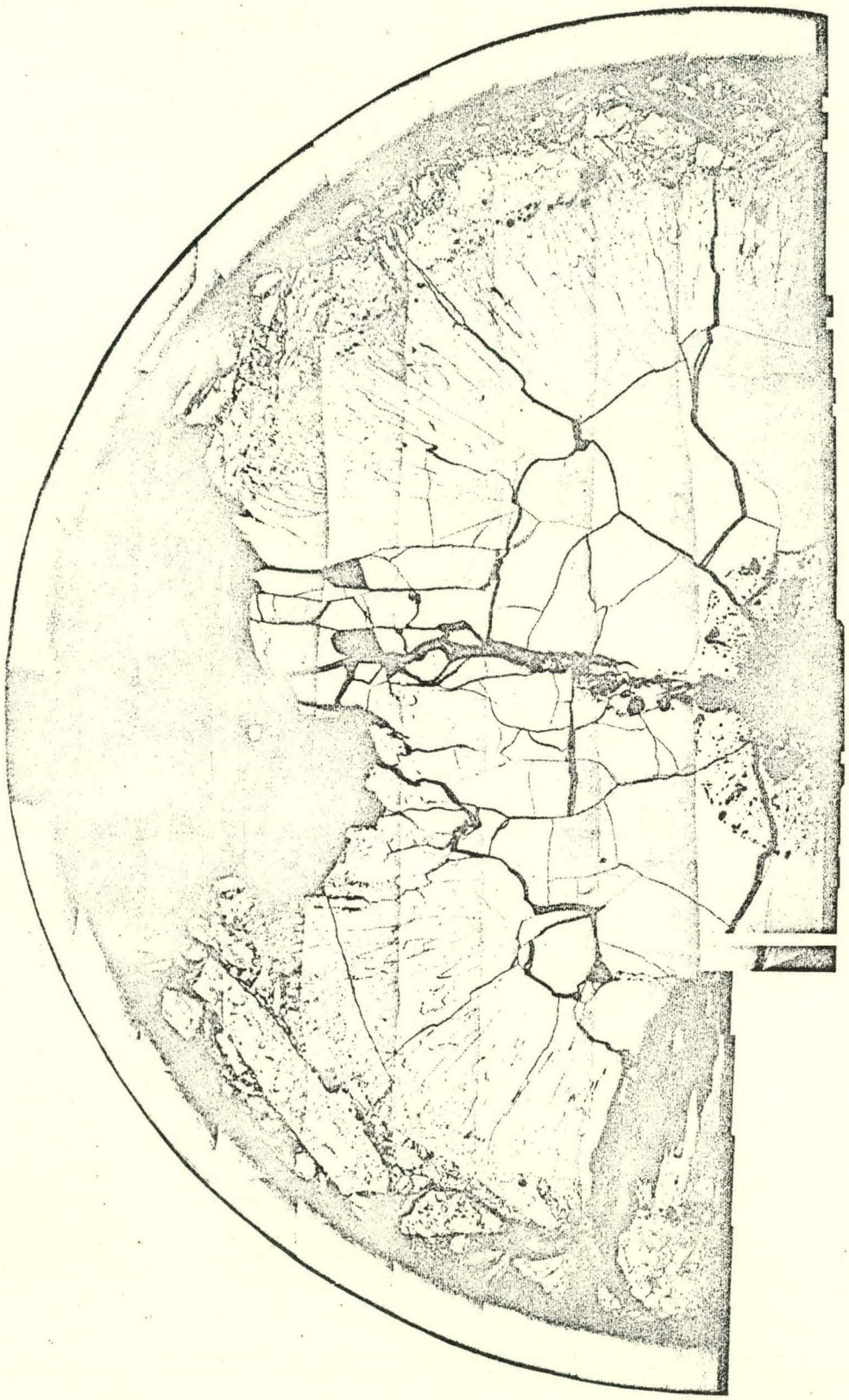

Figure 19. Photomosaic of a Transverse Section Through an Intentionally Defected Vibrationally Compacted UO_2 Fuel Rod. Peak Rod power was approximately 890 w/cm with fuel melting to ∿60% of the radius.

processing equipment. These fuel rod defects characteristically occurred at low burnups (approximately 300 MWd/MTM) because of severe internal hydriding and embrittlement of the cladding by a gas phase hydriding mechanism (Figures 20 and 21). A predominance of the PRTR defects occurred in the end plug crevice region. Laboratory investigations have shown that this crevice region is particularly susceptible to gas phase hydriding attack.[28] Gas phase hydriding type defects are not unique to packed powder fuels since similar defects have been experienced by other investigators in pellet-containing fuel rods.

One of the two defects not attributed to fuel impurities occurred in a swage compacted UO_2 rod and was attributed to cladding damage during swaging. The cause of the other defect in a swage compacted UO_2-PuO_2 rod after a peak burnup of 5800 MWd/MTM has not been determined.[29] This defect was characterized by corrosion on the inside surface of the Zircaloy cladding and a pinhole penetration through the cladding.

Although severe localized embrittlement and loss of cladding fragments occurred in some instances, little or no fuel loss into the coolant resulted and no severe reactor operating difficulties were experienced. Fuel washout or erosion resistance is improved by in-reactor sintering of the packed particle fuel which occurs during the early stages of irradiation at the higher fuel operating temperatures. Water-logging has not been observed in fuel elements that either failed during normal reactor operation or were initially intentionally defected. In many instances, the release of fission product activity was first detected during postshutdown depressurization.

VII. Transient Behavior

The transient behavior or the behavior of fuel subjected to high energy, short duration, power excursions is an important consideration in fuel design and reactor safety. A large number of transient experiments have been performed on pellet type fuel to:

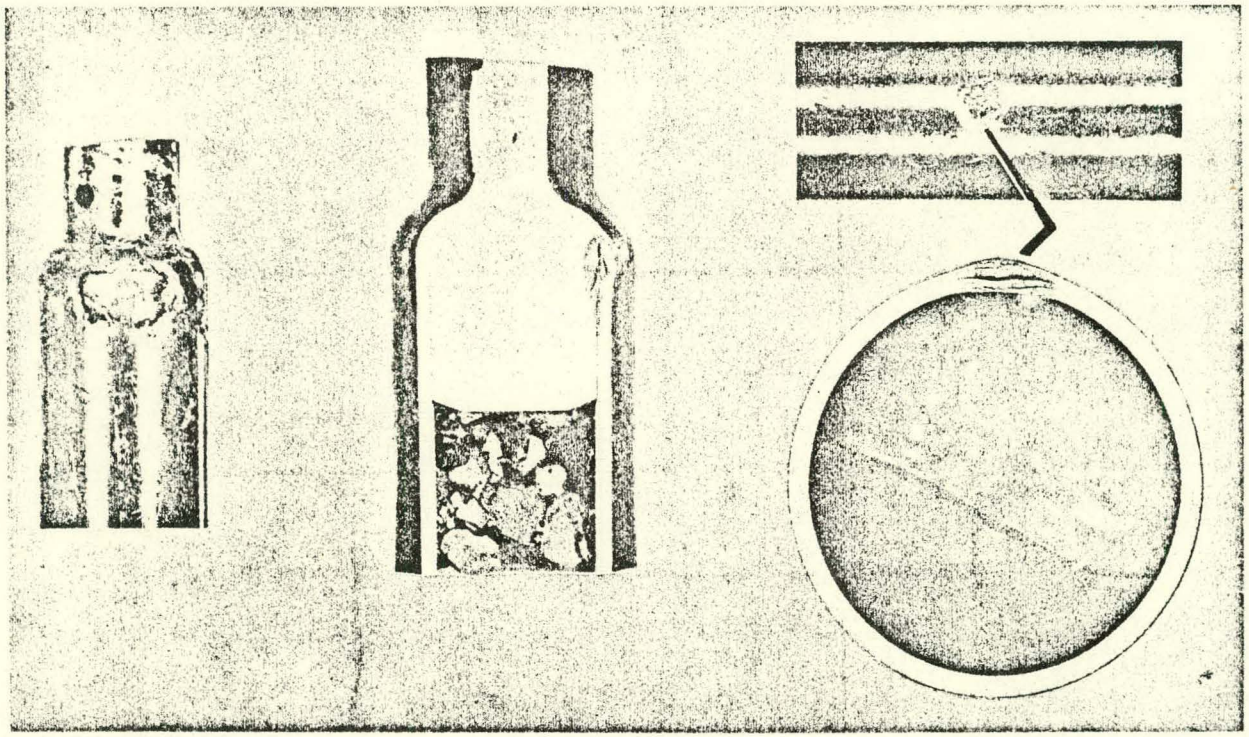

Figure 20

Typical Defects in PRTR Vibrationally Compacted UO_2-PuO_2 Rods Caused by Fuel Contaminates.

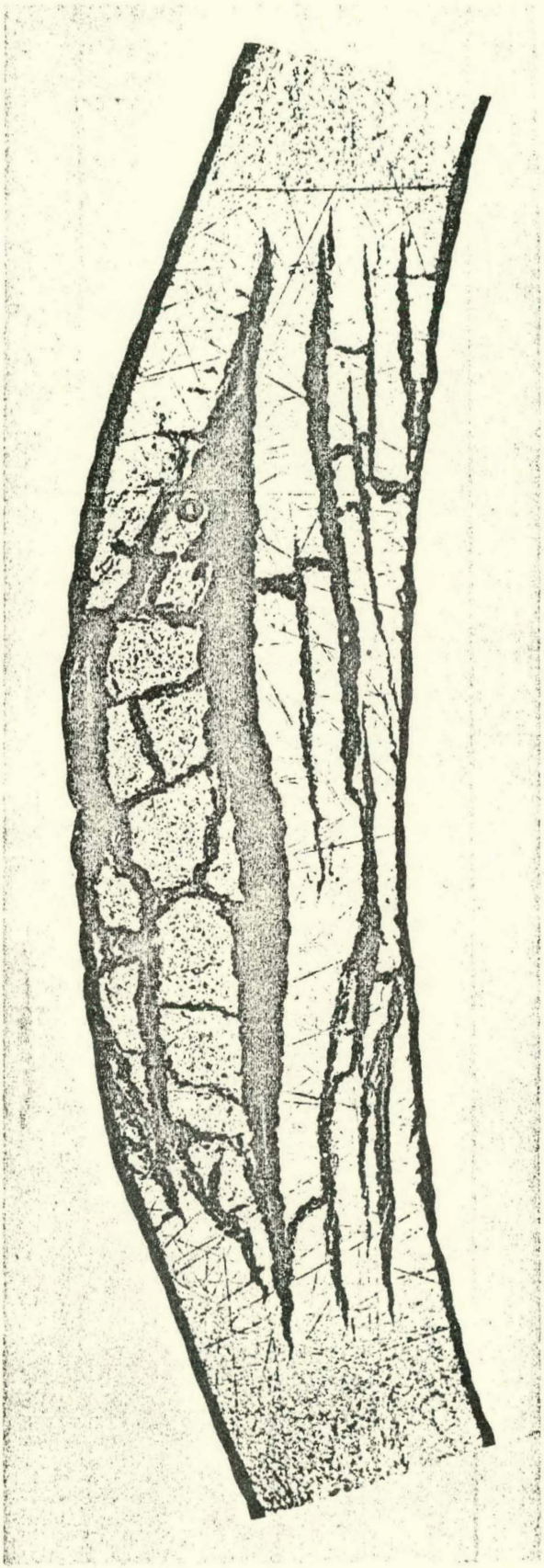

Figure 21
PRTR In-Service Defect

- investigate the extent of metal-water reactions and the fraction of thermal energy converted to mechanical energy.
- investigate the chemical reactivity of dispersed fuel and the nature of the pressure pulse generated.
- establish failure thresholds, failure modes, and possible failure consequences.

Experiments have been conducted with unirradiated vibrationally compacted UO_2 capsules to compare their transient behavior with the behavior of pellet fuels.[30, 31] Two high energy meltdown transient experiments with unirradiated Zircaloy-clad capsules containing vibrationally compacted UO_2 were performed in a water-filled pressure vessel in TREAT.[30] It is not possible to make direct comparisons of the vibrationally compacted fuel data with pellet fuel behavior because the experimental systems and test conditions were not the same. However, there are indications that the extent of $Zr-H_2O$ chemical reaction is approximately the same as previously observed for pellet-containing fuel capsules. There are also indications that the peak pressures attained and the rate of pressure rise in the autoclave during the transient irradiations were higher for vibrationally compacted fuel than for pellet-containing fuel. These more energetic pressure pulses with vibrationally compacted fuel are attributed to the observation that vibrationally compacted UO_2 fragments into smaller particles than pelleted UO_2.

Five experiments were performed with unirradiated vibrationally compacted UO_2 fuel capsules submerged in water under one atmosphere of helium pressure in an apparatus which permitted high speed motion picture recording of capsule behavior while undergoing transient irradiation in TREAT.[31] Comparison of the observations and data obtained from these tests with those of fuel rods containing UO_2 pellets indicates that:

- The fission energy required to produce clad failure in vibrationally compacted fuel rods is between 260 and 330 cal/gm UO_2, which is the same as the energy required to produce clad failure in pelleted fuel rods, i.e., 290 cal/gm UO_2.
- Localized clad bulging was observed with vibrationally compacted fuel rods subjected to fission energies 10 to 20% below that required to cause failure in pelleted UO_2 rods. At threshold, the cladding of pelleted rods failed by melting and no clad bulging was observed.
- These experiments indicate that, in the energy range resulting in clad failure or threshold, the percent of Zr-H_2O chemical reaction is less for vibrationally compacted fuel than for pelleted fuel.

These experiments were performed with unirradiated vibrationally compacted fuel and the results are pertinent to the pre-startup condition with pre-irradiated fuel. In-reactor sintering could have a marked effect on transient behavior.

The significance of the preliminary data obtained from these experiments has prompted further investigations of the transient behavior of vibrationally compacted and pellet-containing fuels under more comparable experimental conditions. Because vibrationally compacted fuel has direct application to plutonium recycle, the possible effects of adding plutonium enrichment to UO_2 in different ways on transient behavior is also being investigated.

1. JJ Hauth and RJ Anicetti, "Vibrational compaction of Ceramic Powders for Nuclear Fuel Elements," HW-SA-1735, October 1959.
2. JJ Hauth, "Vibrational Compaction of Nuclear Fuels," Vibratory Compacting Principles and Methods," Edited by HH Hausner, KH Roll, and PK Johnson, Plenum Press, New York, 1967.
3. JJ Hauth, "Vibration-Compacted Ceramic Fuels," Nucleonics 20 (9): 50-54 (September 1962).
4. FL Brown, LA Neimark, BJ Koprowski, JE Ayer, and JH Kittel, "Performance of Vibratorily Compacted Mixed-Oxide Fuel Rods Under Fast-Reactor Conditions," Trans. Am. Nucl. Soc., Vol. 10, No. 1, P. 101-102 (1967).
5. A Biancheria and RJ Allio, "Fabricating PuO_2-UO_2 Fuels: How Leading Processes Compare," Nucleonics 23 (12): 46-50 (1965).
6. JB Burnham, RE Olson, and MD Freshley, "PuO_2-UO_2 Performance," Nucleonics 24 (2): 83 (1966).
7. RL Richardson, RY Dean, and JJ Hauth, "Theoretical Basis for the Packing of Particles and Application to Nuclear Fuel Elements," BNWL-SA-362, October 1965.
8. RK McGeary, "Mechanical Packing of Spherical Particles," Vibratory Compacting Principles and Methods," Edited by HH Hausner, KH Roll, and PK Johnson, Plenum Press, New York, 1967.
9. CH Bloomster, RE Bardsley, and WT Ross, "An Incremental Loading Process for Controlling Plutonium Enrichment in Mechanically Mixed Oxide Fuel Systems," Trans. Am. Nucl. Soc., Vol. 5, No. 2, p. 452 (1962).
10. "Symposium on Powder Packed Uranium Dioxide Fuel Elements," CEND-153 (November 1962).
11. DW Brite and CA Burgess, "High Energy Rate Pneumatically Impacted UO_2-PuO_2 Fuels," Trans. Amer. Nucl. Soc., Vol. 7, No. 2, p. 408 (1964).

12. Staff of Ceramics Research and Development Operation, "Specifications for Vibrationally Compacted Mixed-Oxide (UO_2-PuO_2) Fuel Elements for the PRTR (Mark I-L), HW-79291, October 1963.
13. JP Keenan and RE Sharp, "PRTR Fuel Element Quality Control System," BNWL-349, January 1967.
14. WG Holmes, "Control of Hydrogen in the Fabrication of Tublular UO_2 Fuel Elements," CEND-153 (Vol. 11), November 1962.
15. "Ceramics Research and Development Operation Quarterly Report, October-December 1964," HW-81603, April 1965.
16. RP Marshall, "Absorption of Gaseous Hydrogen in Zircaloy-2," J Less Common Metals, 13 (1967) 45-52.
17. MD Freshley, FE Panisko, and RE Skavdahl, "The Irradiation Behavior of UO_2-PuO_2 Fuels in PRTR," BNWL-SA-791, 1966 AIME Nuclear Metallurgy Symposium on High Temperature Nuclear Fuels, Delavan, Wisconsin, October 3-5, 1966.
18. MD Freshley and S. Goldsmith, "Operating Experience With Plutonium Fuels in PRTR," Presented at the International Symposium on Plutonium Fuels Technology, October 4-6, 1967, Nuclear Metallurgy, Vol. 13.
19. MD Freshley, TB Burley, and S. Goldsmith, "Plutonium Recycle Fuel Evaluations at PNL," Trans. Am. Nucl. Soc., Vol. 11, No. 2, p. 487-489 (1968).
20. MF Lyons,DH Coplin, H Hausner, B Weidenbaum, and TJ Pashos, "UO_2 Powder and Pellet Thermal Conductivity During Irradiation," GEAT-5100-1, March 1966.
21. DR O'Boyle, FL Brown, and JE Sanecki, "Microanalysis of Solid Fission Products in Mixed-Oxide Fuel Irradiated in EBR-II, Trans. Am. Nucl. Soc., 10 (2), 462-463 (1967).
22. WJ Bailey and MD Freshley, "Irradiation Properties of High Energy Rate Pneumatically Impacted UO_2-PuO_2 Fuels," BNWL-356, April 1967.

23. WJ Baily and TD Chikalla, "Irradiation of Uranium-Plutonium Oxide," Trans. Am. Nucl. Soc., Vol. 6, No. 2, p. 350 (1963), HW-SA-3129.
24. RM Carroll and O. Sisman, Reactor Chemistry Division Annual Progress Report for Period Ending January 31, 1965, ORNL-3789, Oak Ridge, Tennessee, p. 223.
25. TB Burley and MD Freshley, "Internal Gas Pressure Measurements in PRTR Mixed-Oxide Fuel Rods," Trans. Am. Nucl. Soc., Vol. 11, No. 1, p. 106-107 (1968).
26. MD Freshley and FE Panisko, "The Irradiation Behavior of UO_2-PuO_2 Fuels in PRTR," BNWL-366, March 1967.
27. MD Freshley, RG Wheeler, JM Batch, and GM Hesson, "Investigation of the Combined Failure of a Pressure Tube and Defected Fuel Rod in PRTR," BNWL-272, May 1966.
28. "Ceramics Research and Development Operation, Quarterly Report, October-December 1964," HW-81603, April 1965, p.4.9.
29. "Ceramics Research and Development Operation, Quarterly Report, April-June 1964," HW-81601, November 1964, p. 4.2.
30. RC Liimatainen, MD Freshley, and FJ Testa, "Transient Irradiations of Vibrationally Compacted UO_2 Fuel in TREAT," Trans. Am. Nucl. Soc., Vol. 9, No. 2, p.395-396 (1966).
31. RG Gulley, DR Armstrong, and JL Harrison, "Transient Irradiation Experiments With Vibrationally Compacted UO_2 Fuel Rods in TREAT," Trans. Am. Nucl. Soc., Vol. 11, No. 1, p. 111-112 (1968).